General Disclaimer

One or more of the Following Statements may affect this Document

- This document has been reproduced from the best copy furnished by the organizational source. It is being released in the interest of making available as much information as possible.

- This document may contain data, which exceeds the sheet parameters. It was furnished in this condition by the organizational source and is the best copy available.

- This document may contain tone-on-tone or color graphs, charts and/or pictures, which have been reproduced in black and white.

- This document is paginated as submitted by the original source.

- Portions of this document are not fully legible due to the historical nature of some of the material. However, it is the best reproduction available from the original submission.

9950-981

THREE DIMENSIONAL RAY TRACING OF THE JOVIAN MAGNETOSPHERE IN THE LOW FREQUENCY RANGE

SwRI PROJECT NO. 15-6546
JPL CONTRACT NO. 956026

FINAL REPORT

MAY 1984

J.D. MENIETTI

SOUTHWEST RESEARCH INSTITUTE
P.O. DRAWER 28510
SAN ANTONIO, TX 78284

THREE DIMENSIONAL RAY TRACING

OF THE

JOVIAN MAGNETOSPHERE IN THE LOW FREQUENCY RANGE

SwRI PROJECT NO. 15-6546
JPL CONTRACT NO. 956026

FINAL REPORT

MAY 1984

J.D. MENIETTI

SOUTHWEST RESEARCH INSTITUTE
P.O. DRAWER 28510
SAN ANTONIO, TX 78284

THREE DIMENSIONAL RAY TRACING OF THE JOVIAN MAGNETOSPHERE IN THE LOW FREQUENCY RANGE

SwRI Project No. 15-6456
JPL Contract No. 956026

Final Report

April 1984

J. D. Menietti
Southwest Research Institute
P. O. Drawer 28510
San Antonio, TX 78284

This work was performed for the Jet Propulsion Laboratory, California Institute of Technology, sponsored by the National Aeronautics and Space Administration under Contract NAS7-100.

TABLE OF CONTENTS

TABLE OF CONTENTS

I. SUMMARY

The investigative efforts at Southwest Research Institute have centered on the development and execution of a comprehensive three-dimensional ray tracing code. This code contains a model of the Jovian magnetosphere which includes the O-4 magnetic field description (Acuna and Ness, 1976) and an empirical plasma model. Decametric radiation (2-35MHz) has been the primary subject of the analyses but some studies in the whistler mode (< 10kHz) have been performed. The whistler mode analyses yielded the approximate dimensions of Jovian lightning source regions and the approximate energy dispersion. From the latter an estimate of the Jovian lightning emission rate was made. These results were previously reported in the Final Report submitted to the Jet Propulsion Laboratory in October, 1982. The decametric radiation (DAM) studies have produced numerous publishable results.

The early work of the current contract in ray tracing of DAM did not incorporate a model Jovian ionosphere. Sources were assumed to be at the foot of the Io flux tube and only northern hemisphere sources were initially considered. Emission emanating in a hollow cone around the active field line was ray traced from sources separated by 10° in Jovian longitude. One of the most notable results was the observation that not only does the magnetic field model control the frequency extent of the emission but also the curvature and morphology of the arcs. The importance of displaying the Planetary Radio Astronomy data in a constant-Io longitude format were clearly demonstrated in this early work. The results were published in the Journal of Geophysical Research (Appendix 1).

Isolated, high-curvature DAM arcs were modelled by varying the wave normal angle at the source until the ray tracing results matched the observations. Plots of wave normal angle versus frequency for different

Doppler shifts at the source were made which provide the first comprehensive three-dimensional description of the relationship of these variables. The results were compared with the theoretical work of Staelin (1981) and imply a maximum wave normal angle of about 80° for the high-curvature arcs. This work has been submitted to the Journal of Geophysical Research (Appendix 3).

Because the Jovian ionosphere was found to strongly influence the higher frequency radiation, an empirical expression was used to represent the ionosphere in the code. The ray tracing of Jovian DAM source points was repeated including the southern hemisphere sources. The results have, for the first time clearly delineated northern and southern hemisphere sources in the Voyager data. The southern hemisphere arcs are lower in frequency extent and have a narrower emission cone angle. These findings lend strong support to the theory that arc morphology is primarily a result of wave refraction in the magnetosphere rather than emission processes. Appendix 2 is preprint of a paper submitted to the Journal of Geophysical Research detailing these exciting results.

The next step in reformatting the Voyager data led to a discovery of an Io-independent emission which is most probably the Jovian counterpart to terrestial auroral kilometric radiation (AKR). By plotting the sub-Io longitude versus the difference between the spacecraft and the sub-Io longitude, an emission which has been named Jovian Auroral Decametric Radiation (JADR) has been identified. This emission appears to emanate only from high-latitude nightside auroral zone sources in a manner similiar to the terrestial AKR. These results have been submitted to the Journal of Geophysical Research and appear in preprint form in Appendix 4.

II. INTRODUCTION

This work represents culmination of a three year activity involving ray tracing studies of Jovian low frequency emisions. The program included the development and execution of a comprehensive three-dimensional ray tracing computer code for examination of model Jovian decametric (DAM) emission. A detailed description of this program has been submitted to the Jet Propulsion Laboratory as "Final Report" dated October, 1982. In the present report a brief description of the improvements to the computer code will be outlined and a presentation of the results of ray tracing of Jovian emissions will be presented in the form of summaries with details given in the appendices. The appendices contain copies of papers that have been accepted or submitted for publication to the Journal of Geophysical Research.

III. TECHNICAL DISCUSSION

A. Previous Results

As described previously in the "Final Report" dated October, 1982 (hereafter referred to as FR1982), DAM emission from northern hemisphere source positions located at the feet of Io flux tubes separated by 10° in Jovian longitude have been ray traced. The results were compared to Voyager 1 and 2 observations and have been published in the Journal of Geophysical Research. As a result of these efforts the importance of wave propagation effects in reproducing the observed Jovian DAM arcs became apparent. The magnetic field model and ionospheric effects were seen to be fundamentally important. In addition, the arcs were seen to be divided into high and low curvature classes. Initial explanations for some of the differences between these classes were presented which included variations of initial wave normal angle and local magnetic field strength at the source. Appendix I is a reprint of a paper published in the Journal of Geophysical Research entitled "Three Dimensional Ray Tracing of Jovian Radiation in the Low Frequency Range" which details the results of this original work.

Initial studies of whistler mode emissions (1-3kHz) from lightning sources in the Jovian cloud tops were also made as discussed in FR1982. Whistlers were ray traced through the Jovian magnetosphere and into the Io torus in an effort to determine the extent of the source positions and the degree of energy dissipation from this emission. These results have been reported to the University of Iowa and are awaiting submission for publication.

B. Improvements to the Computer Code

As detailed in FR1982, the ray tracing code is based on the Stix cold plasma formulation and solves the Haselgrove (1954) equations for the index of refraction. The method of solution is by Runge-Kutta integration with a modified Hamming predicator/corrector scheme. The ambient Jovian plasma density model is based on the Sentman-Goertz empirical results and the Io torus plasma density is a spline fit to the published contours of Warwick et al. (1979). The magnetic field model used is the O-4 model of Acuna and Ness (1976). Now included in the code is an ionospheric model based on the empirical nonlinear fitting of Hashimoto and Goldstein, (1983).

Atreya and Donahue, 1976 have derived a model Jovian ionosphere based on observations. Hashimoto and Goldstein, (1983) have used a nonlinear least squares fit to the model of Atreya and Donahue producing the following analytical result:

$$N_I = 1.15 \times 10^5 \exp((1417-h/386.3)/(1+(991/(h-276))^{4.31}),$$

where $N_I(cm^{-3})$ is the ionospheric electron density, h is the altitude in km above the cloud tops and $N_I=0$ for $h < 276$ km. The magnetospheric model and the ionospheric models have been matched at the top of the ionosphere so that a smooth transition occurs. With the addition of the ionosphere it was necessary to ray trace DAM at all frequencies whose source positions reached the ionosphere.

In order to display the results of the ray tracing code a plot program was developed on an HP1000 computer which provided high quality ink bed plots. The wave frequency versus Jovian system III longitude was displayed on these plots with sources for each sub-Io longitude clearly indicated by color symbols. This plotting technique allowed easy comparison of the model arcs with Voyager 1 and 2 observations.

C. New Results

As a result of the identification of the Jovian ionosphere as an important source of wave refraction at certain DAM frequencies, it was necessary to ray trace all the northern hemisphere DAM source positions again. The results of Staelin, (1981) suggested a constant initial wave normal angle of 85° at the source (instead of the original 90° used in the previous study [cf. Appendix 1]). Figure 1 (A-D) shows the resulting model emission on a frequency-versus-system III-longitude scale for arcs within the longitude ranges of 10°-90°, 100°-180°, 190°-270°, and 280°-360° respectively. Figure 2 is in the same format for the source points of the southern hemisphere. It is immediately apparent that the model southern hemisphere source emissions have a lower frequency cutoff than the northern hemisphere sources, and emission cone edges are closer together in longitude. In order to directly compare the model ray tracing results with actual observations it was decided to re-format the Voyager 1 and 2 Planetary Radio Astronomy (PRA) data by sorting it with a fixed sub-Io longitude. This allowed direct comparison with the ray tracing results. The reformatted data was obtained from Marshall Space Flight Center as a result of the efforts of J. L. Green and N. F. Six, supported by the Jupiter Data Analysis Program. Comparison of the model and observations was very good for some cases and allowed the first delineation of Jovian DAM emissions into southern and northern hemisphere sources. A detailed discussion of the comparison is included in this report as Appendix 2, which is a preprint of a paper entitled "Identification of Decametric Radiation From Sources in the Southern Hemisphere of Jupiter" submitted for publication to the Journal of Geophysical Research.

Careful study of the dynamic frequency-time Voyager spectrograms reveals a multitude of arc morphologies with arcs varying in frequency extent and in curvature. Included is a class of arc with large frequency extent and curvature which appears often as intense, and somewhat isolated from the surrounding arcs. By assuming a wave normal angle which varied with frequency at the source point we were able to match the curvature of these observed high-curvature arcs with model ray tracing results. The wave normal angles chosen were consistent with relativistically Doppler-shifted electron emission in RX mode (Staelin, 1981). The electron energy was found to be about 6 keV which is in agreement with electron energies in the vicinity of the Io torus which are hypothesized to be accelerated and produce the DAM. This work represents the first comprehensive three-dimensional ray tracing analysis of varying the wave normal angle. Previous studies considered only a two-dimensional analysis and consequently could not adequately reproduce observed arcs. The results of the present analysis are detailed in Appendix 3 which is a preprint of a paper entitled "Jovian Decametric Arcs: An Estimate of the Required Wave Normal Angles From Three-Dimensional Ray Tracing", submitted to the Journal of Geophysical Research.

The reformatting of the Voyager PRA data has allowed rapid analysis of both Io-dependent and Io-independent emissions. Carrying the process one step further, S. Gulkis plotted the data using the sub-Io longitude as the ordinate and the difference between the spacecraft longitude and the sub-Io longitude as the coordinate. This technique immediately allowed the identification of an Io-independent emission which has been named Jovian Auroral Decametric Radiation (JADR). This radiation is seen only on the nightside and appears to have a source in the high-latitude auroral zone. These facts indicate the emission may be the Jovian counterpart to the

intensely studied terrestial AKR emissions. Appendix 4 is a preprint of a paper entitled "Identification of a Night-Side Component of DAM as a Jovian Counterpart to AKR" submitted to the Journal of Geophysical Research which details the exciting discovery.

IV. CONCLUSIONS

Results of three-dimensional ray tracing of Jovian low frequency radiation have provided important information regarding the propagation of DAM emissions. Direct comparison of model ray tracing results with observed arcs has indicated that many arcs can be adequately explained by propagation from hollow emission cones with sources at the feet of Io flux tubes. Emission occurs at frequencies slightly Doppler-shifted above the RX cutoff frequency, with wave normal angles close to 90°. In addition, the effect of the magnetic field in determining the curvature and frequency extent of the arcs is fundamental (cf. Appendix 1).

After the introduction of a Jovian ionospheric model new ray tracing results have yielded improved model arcs for the northern hemisphere and the first three-dimensional model arcs with source positions in the southern hemisphere (Appendix 2). The ray tracing has allowed the first delineation of northern and southern hemisphere emissions of Voyager data. The importance of re-formatting the Voyager data such that the sub-Io longitude can be held fixed has been found to be of fundamental importance in determining Io-dependent spectral features.

Certain high-curvature arc signatures can be modelled by allowing the wave normal angle to vary yielding a $\Psi(f)$ relationship that is unique to the high-curvature arcs. One explanation for the smaller wave normal angles necessary to model certain high-curvature arcs is relativistically Doppler-shifted electron gyro-emission (Appendix 3). For electrons with energies of about 10 keV (reasonable for the source particles) the wave normal angles resulting from theoretical Doppler shifted emission are quite close to the values obtained from ray tracing needed to match the observed arcs. The implication is that certain high-curvature arcs result from the gyro-emission of beamed electrons with energies of a few keV.

Reformatting the Voyager PRA data has also allowed the identification of an Io-independent emission which is the probable couterpart to the terrestial AKR. Jovian Auroral Decametric Radiation may provide new insights to the emission mechanism responsible for the production of AKR, as well as provide valuable information about the structure of the Jovian magnetosphere.

REFERENCES

Acuna, M. A., and N. F. Ness, "The Main Magnetic Field of Jupiter", J. Geophys. Res., 81, 2917, 1976.

Atreya, S. K. and T. M. Donahue, "Model Ionospheres of Jupiter", in Jupiter, edited by T. Gehrels, p. 304, University of Arizona Press, Tucson, 1976.

Haselgrove, J., "Ray Theory and a New Method of Ray Tracking", in Report of Conference on the Physics of the Ionosphere, pp. 355-364, London Physical Society, London, 1955.

Hashimoto, K. and M. L. Goldstein, "A Theory of the Io Phase Asymmetry of the Jovian Decametric Radiation", J. Geophys. Res., 88, 2010, 1983.

Sentman, D. D., and C. K. Goertz, "Whistler Mode Noise in Jupiter's Inner Magnetosphere", J. Geophys. Res., 83, 3151, 1978.

Staelin, D. H., "Character of the Jovian Decametric Arcs", J. Geophys. Res., 86, 8581, 1981.

Stix, T. H., The Theory of Plasma Waves, pp. 5-34, McGraw-Hill, New York, 1962.

Warwick, J. W., J. B. Pearce, A. C. Riddle, J. K. Alexander, M. D. Desch, M. L. Kaiser, J. R. Thieman, T. D. Carr, A. Boischot, C. C. Harvey, and B. M. Pederson, "Voyager 1 Planetary Radio Astronomy Observations Near Jupiter", Science, 204, 995, 1979.

FIGURE CAPTIONS

FIGURE 1: Frequency versus system III '65 longitude showing the model arcs at 10° intervals of constant Io CML. The Io CML is labelled on each curve. The curves represent the intersection of one "side" of the emission cone with a radial shell at 150 R_j. The source points for the arcs shown lie on Io flux tubes in the northern hemisphere with longitudes in the range: A) 10° to 90°; B) 100° to 180°; C) 190° to 270°; and D) 280° to 360°.

FIGURE 2: Same as Figure 1 except the source points for the arcs shown lie on Io flux tubes in the SOUTHERN hemisphere with longitudes in the range: A) 10° to 90°; B) 100° to 180°; C) 190° to 270°; and D) 280° to 360°.

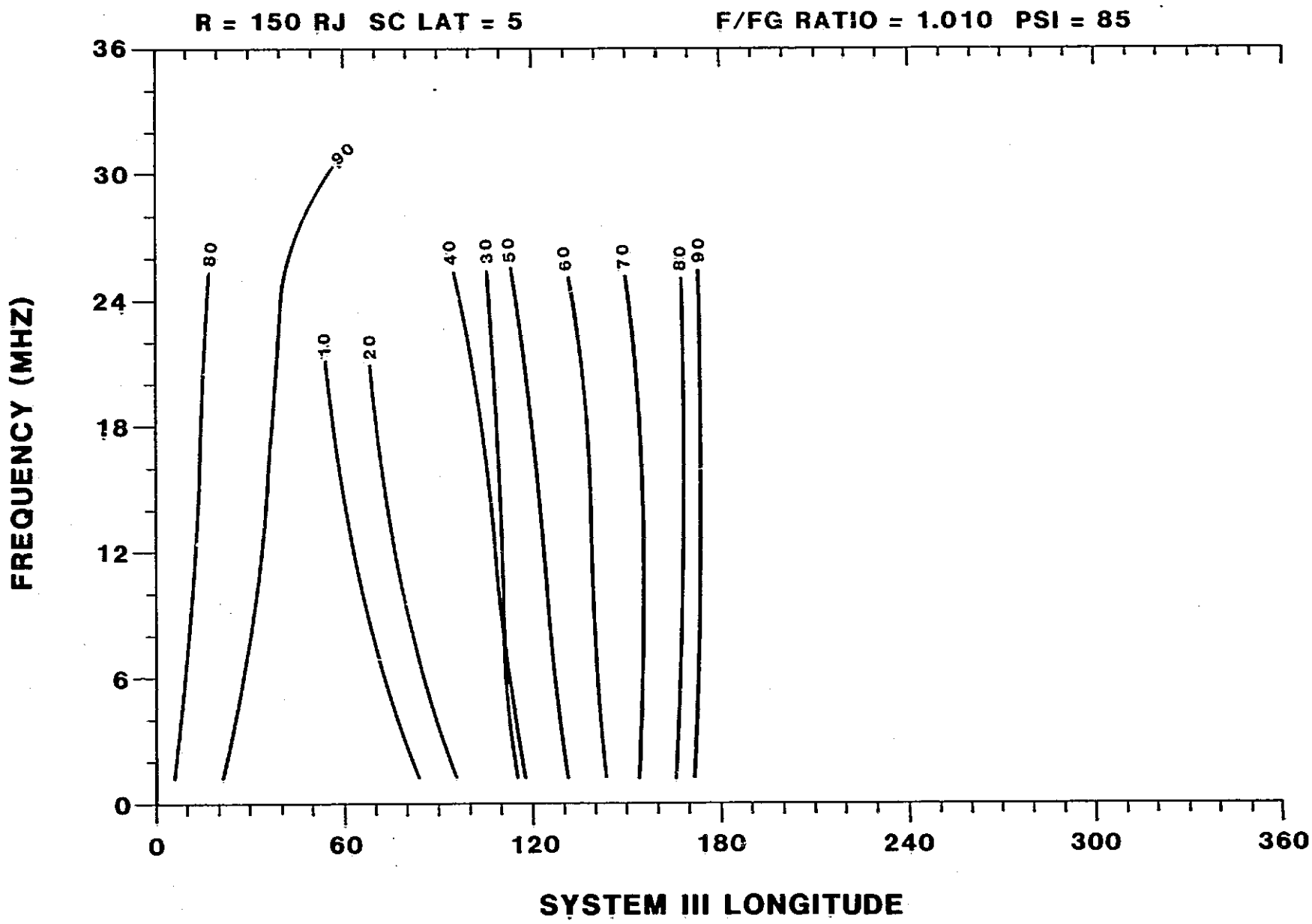
R = 150 RJ SC LAT = 5
F/FG RATIO = 1.010 PSI = 85
FREQUENCY (MHZ)
36
30
24
18
12
6
0
0
60
120
180
240
300
360
SYSTEM III LONGITUDE
80
90
10
20
40
30
50
60
70
80
90

FIGURE 1A

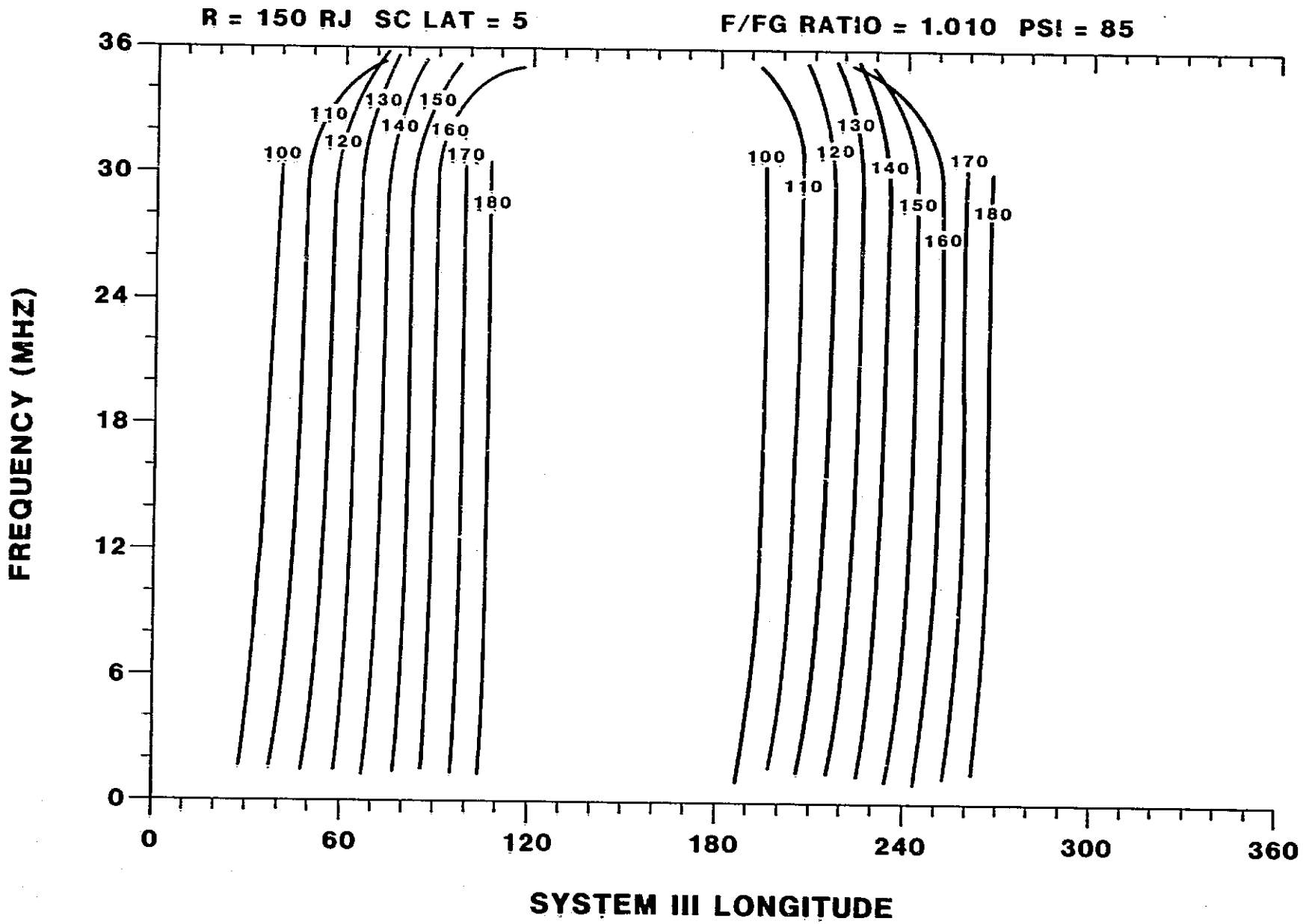
R = 150 RJ SC LAT = 5
F/FG RATIO = 1.010 PSI = 85
FREQUENCY (MHZ)
SYSTEM III LONGITUDE
0
6
12
18
24
30
36
0
60
120
180
240
300
360
100
110
120
130
140
150
160
170
180

FIGURE 1B

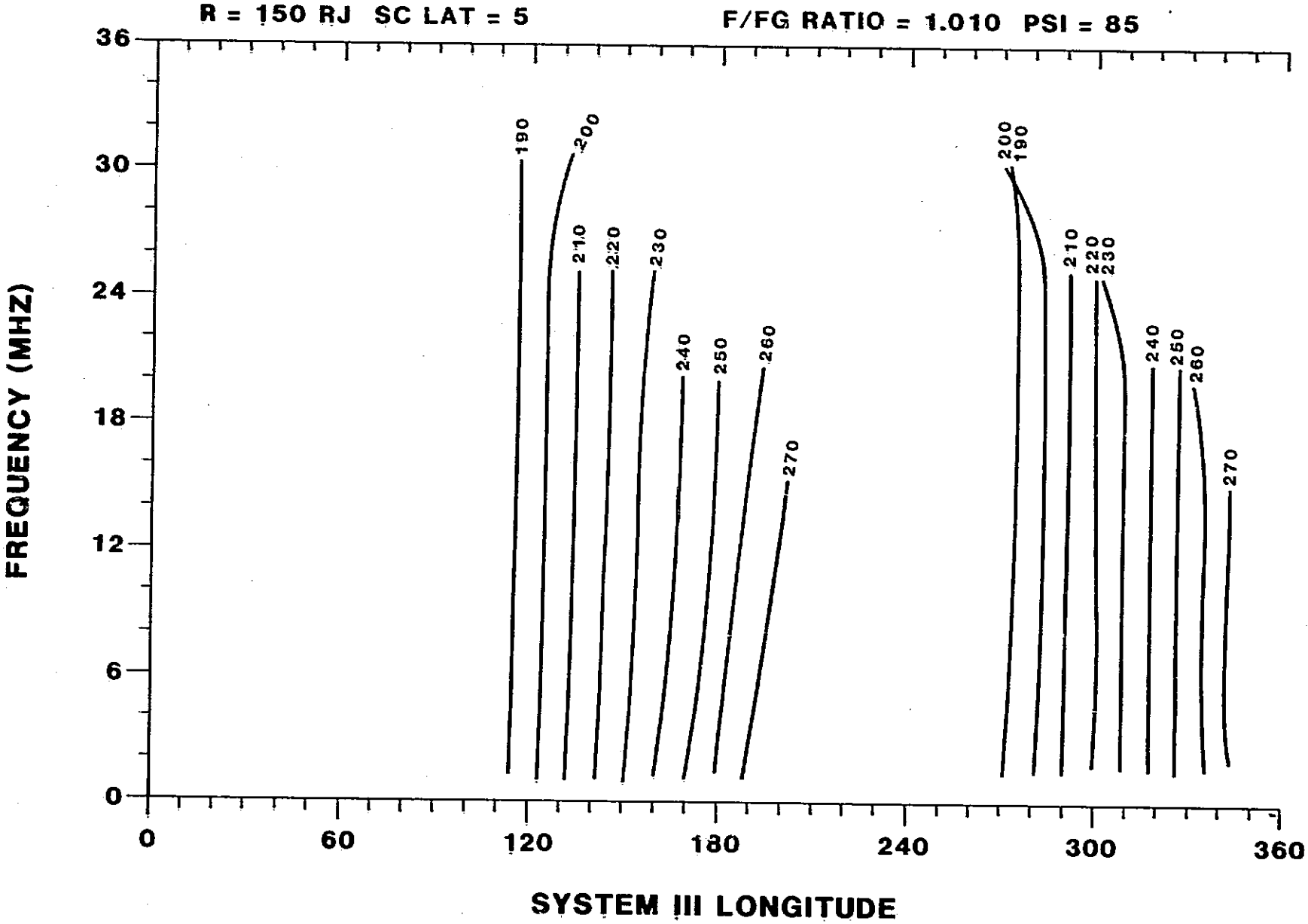
R = 150 RJ SC LAT = 5
F/FG RATIO = 1.010 PSI = 85
FREQUENCY (MHZ)
36
30
24
18
12
6
0
0
60
120
180
240
300
360
SYSTEM III LONGITUDE
190
200
210
220
230
240
250
260
270
200
190
210
220
230
240
250
260
270

FIGURE 1C

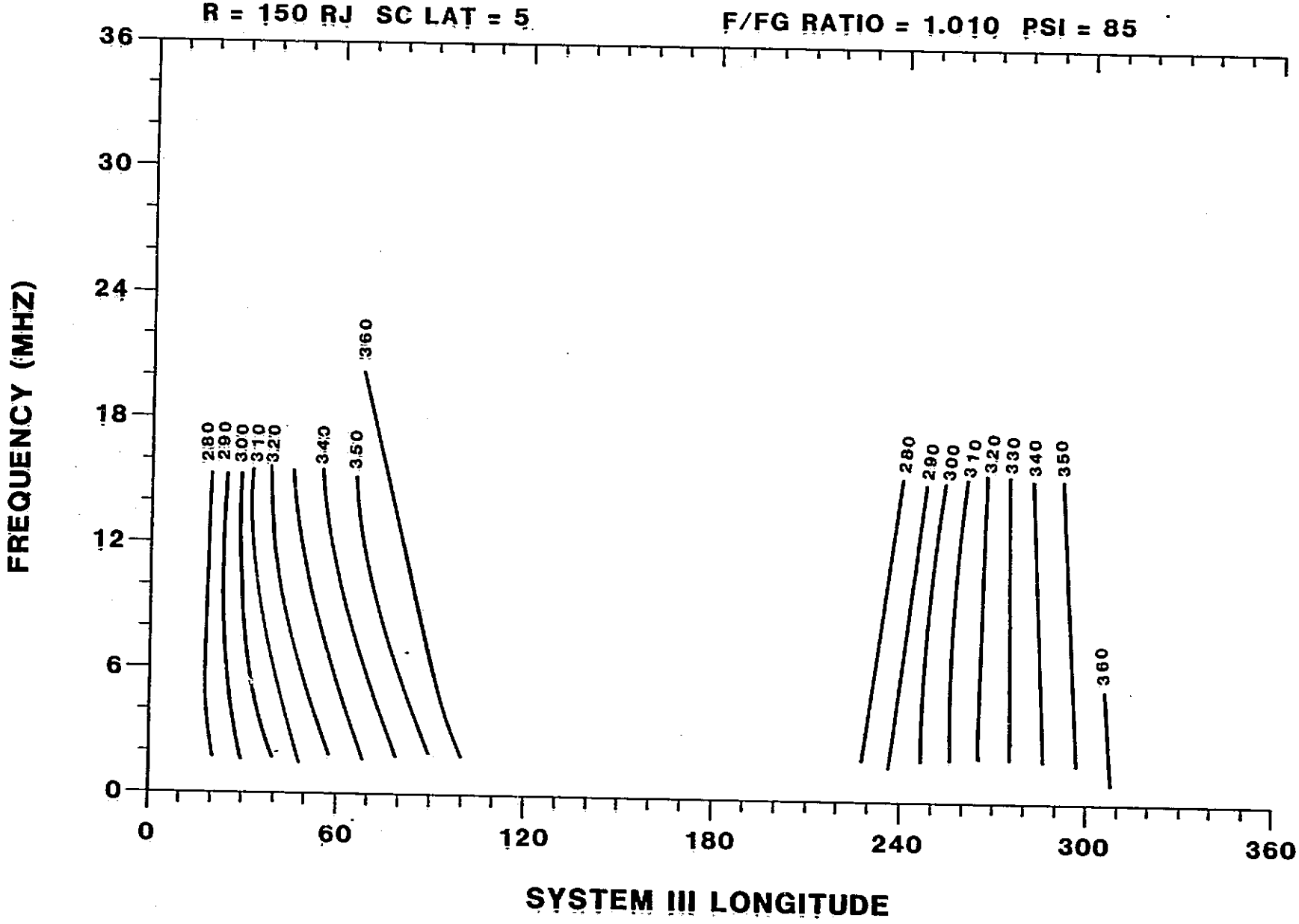
R = 150 RJ SC LAT = 5
F/FG RATIO = 1.010 PSI = 85
FREQUENCY (MHZ)
36
30
24
18
12
6
0
0
60
120
180
240
300
360
SYSTEM III LONGITUDE
280
290
300
310
320
340
350
360
280
290
300
310
320
330
340
350
360

FIGURE 1D

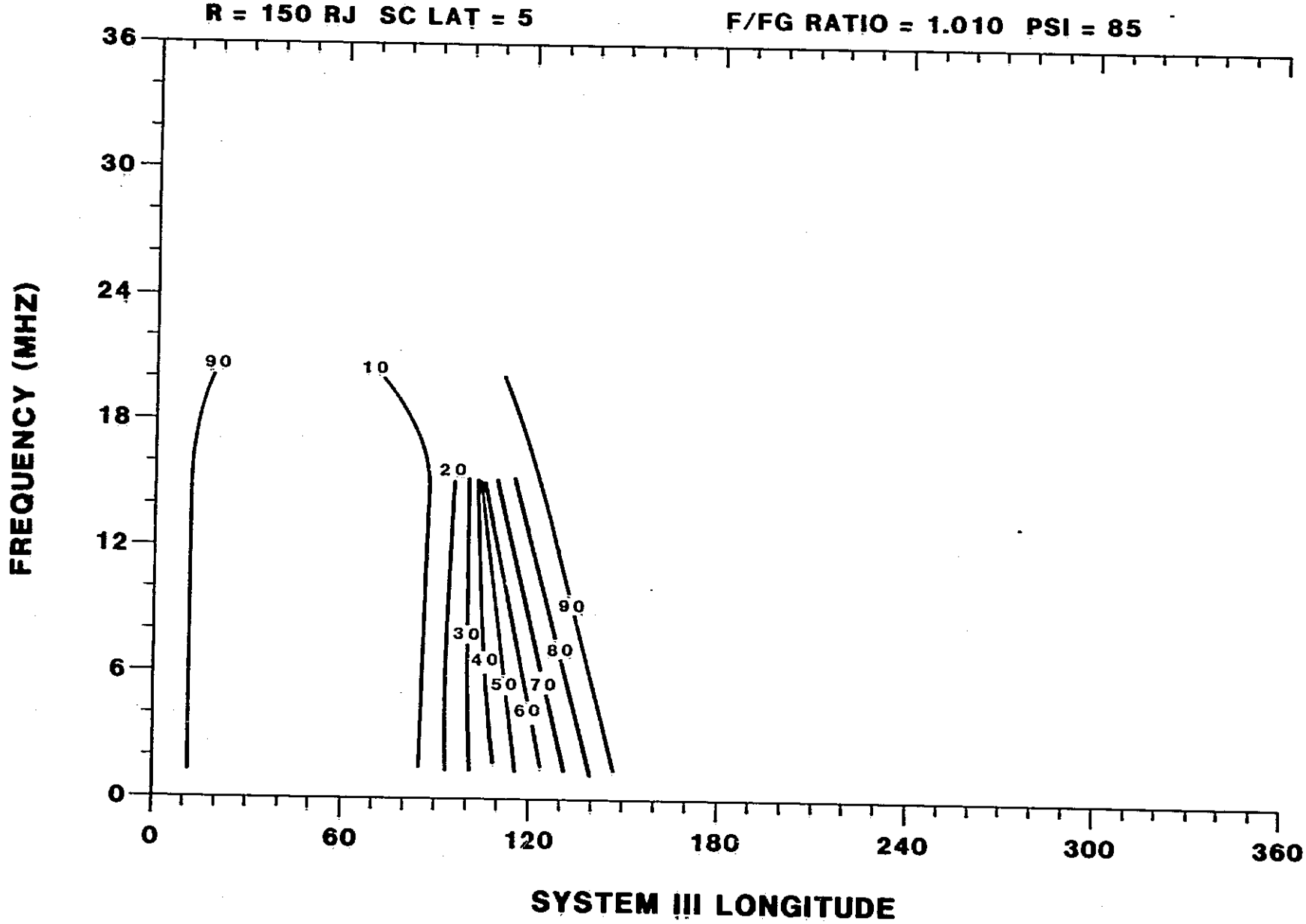
R = 150 RJ SC LAT = 5
F/FG RATIO = 1.010 PSI = 85
FREQUENCY (MHZ)
36
30
24
18
12
6
0
0
60
120
180
240
300
360
SYSTEM III LONGITUDE
90
10
20
30
40
50
60
70
80
90

FIGURE 2A

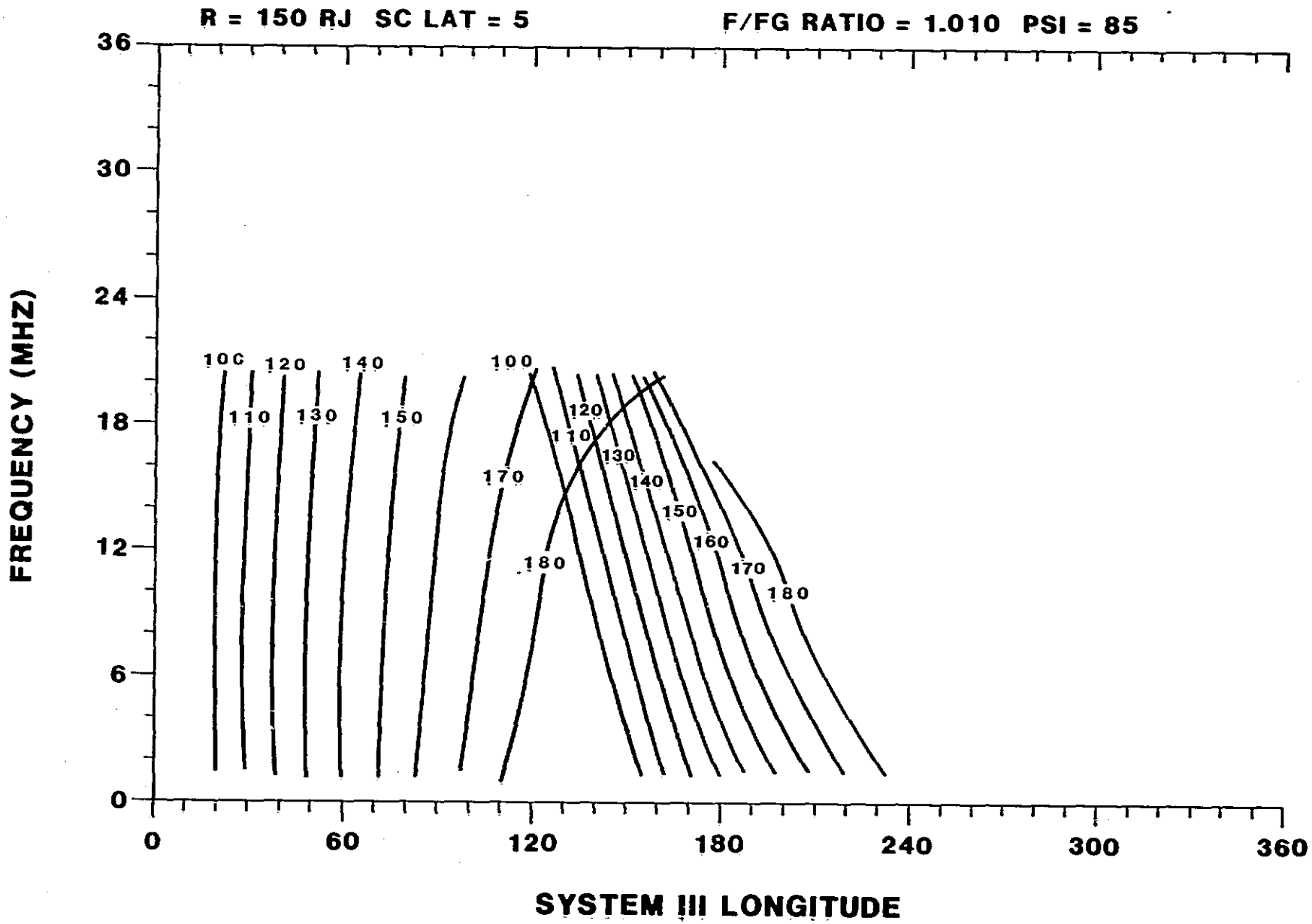
R = 150 RJ SC LAT = 5
F/FG RATIO = 1.010 PSI = 85
FREQUENCY (MHZ)
36
30
24
18
12
6
0
0
60
120
180
240
300
360
SYSTEM III LONGITUDE
100
110
120
130
140
150
170
180
100
120
110
130
140
150
160
170
180

FIGURE 2B

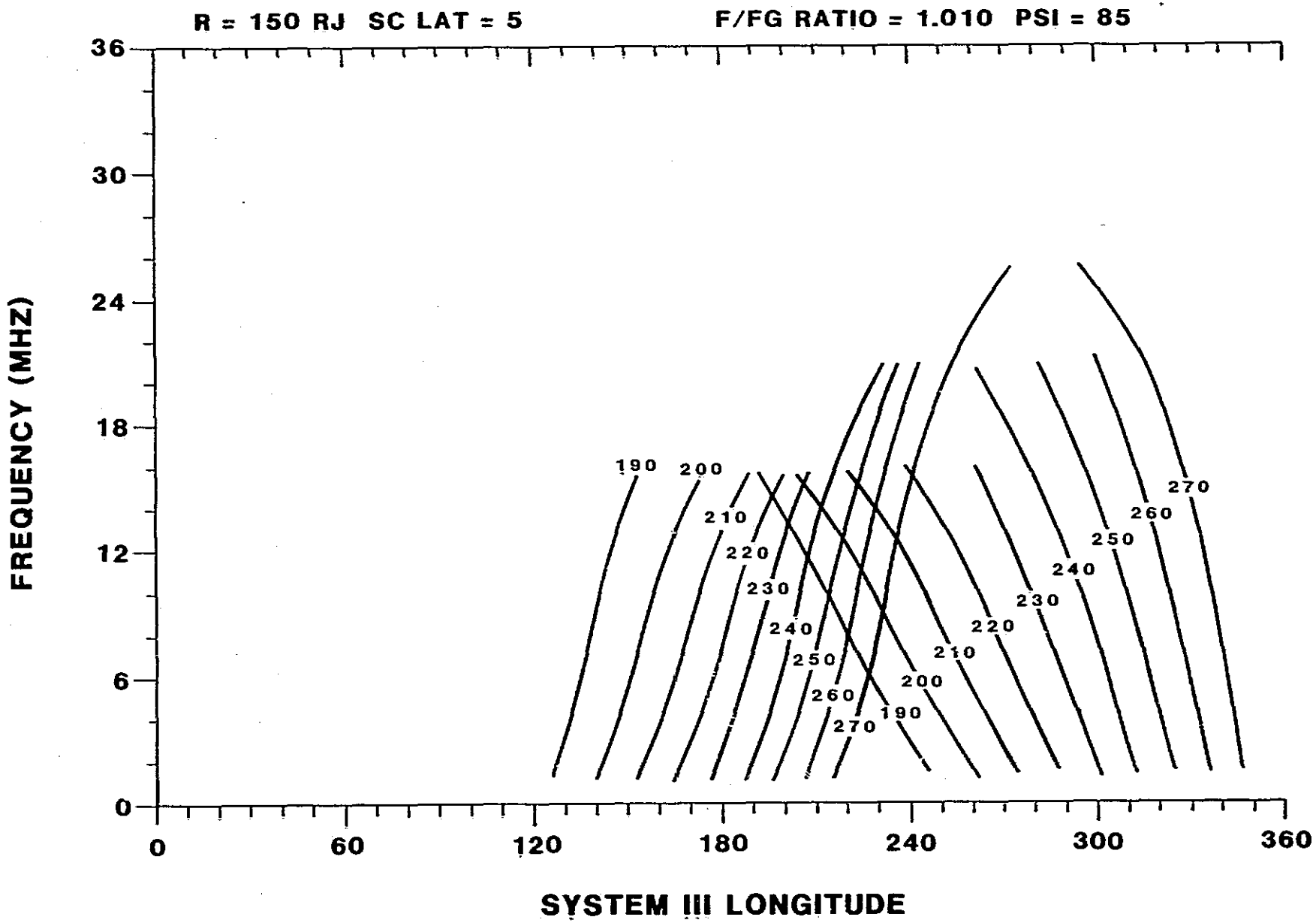
R = 150 RJ SC LAT = 5
F/FG RATIO = 1.010 PSI = 85
FREQUENCY (MHZ)
36
30
24
18
12
6
0
0
60
120
180
240
300
360
SYSTEM III LONGITUDE
190
200
210
220
230
240
250
260
270

FIGURE 2C

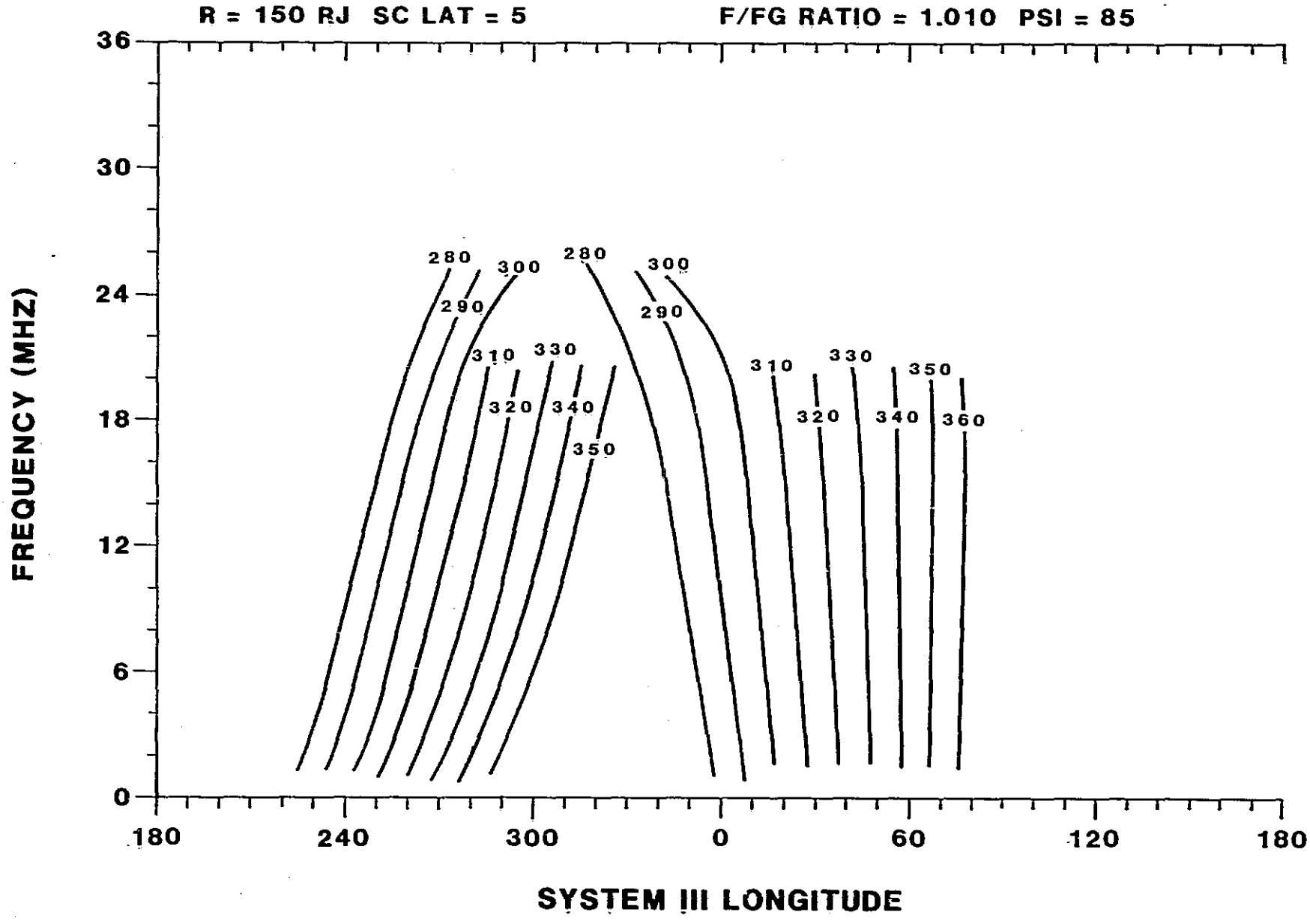
R = 150 RJ SC LAT = 5
F/FG RATIO = 1.010 PSI = 85
FREQUENCY (MHZ)
36
30
24
18
12
6
0
280
290
300
310
320
330
340
350
360
180
240
300
0
60
120
180
SYSTEM III LONGITUDE

FIGURE 2D

VII. APPENDICES

A. Appendix 1: "Three-Dimensional Ray Tracing of Jovian Radiation in the Low Frequency Range"

JOURNAL OF GEOPHYSICAL RESEARCH, VOL. 89, NO. A3, PAGES 1489-1495, MARCH 1, 1984

Three-Dimensional Ray Tracing of the Jovian Magnetosphere in the Low-Frequency Range

J. D. MENIETTI,[1] J. L. GREEN,[2] S. GULKIS,[3] AND F. SIX[4]

Three-dimensional ray tracing of the Jovian DAM emission has been performed utilizing the O-4 magnetic field model (Acuna and Ness, 1979) and a realistic plasma model. Minimal assumptions about the emission mechanism have been made that include radiation in the right-hand extraordinary mode, propagating nearly perpendicular to the field line at source points located just above the RX cutoff frequency along Io flux tubes. We have performed ray tracing in the frequency range from 2-35 MHz from successive Io flux tubes separated by ten degrees of central meridian longitude for a full circumference of northern hemisphere sources. Our results show unusual complexity in model arc spectra that is displayed in a constant Io phase format with many similarities to the Voyager PRA data. The results suggest much of the variation in observed DAM spectral features is a result of propagation effects rather than emission process differences. We feel our work represents a comprehensive ray tracing investigation of DAM arc emission and presentation of the results in a unique format.

INTRODUCTION

One of the most characteristic features of the Jovian decametric radio emissions is the presence of arc-like structures in frequency-time spectrograms. The arc-like structures were first observed by the Voyager planetary radio astronomy experiment (PRA) [*Warwick et al.*, 1979] and later found in ground based observations [*Boischot et al.*, 1981]. The arcs consist of narrow band emissions that drift in frequency in a repeatable and highly organized manner as shown in Plate 1. The frequency range of the arc emission is from 40 MHz down to several MHz or lower, but all arcs do not span this full frequency range. Several different kinds of arcs have been recognized in the data, depending on their curvatures, which either open toward increasing time (vertex early) or open toward decreasing time (vertex late). The arcs often appear as a closely spaced series referred to as "nested arcs." Detailed descriptions of the arcs can be found elsewhere [i.e., *Warwick et al.*, 1979; *Leblanc*, 1981; *Boischot and Aubier*; 1981, *Carr et al.*, 1983].

Various source mechanisms have been proposed to explain the decametric arcs. A general feature of most theories is that the emission occurs along conical sheets that are swept past the observer as the planet rotates as first suggested by *Dulk* [1965]. Many investigators attribute the emission to precipitating electrons along the Io magnetic flux tube that radiate near the gyrofrequency [*Goldreich and Lynden-Bell*, 1969; *Smith*, 1976; *Goldstein and Goertz*, 1983]. *Goldstein and Theiman* [1981], *Pearce* [1981], *Staelin* [1981], *Neubauer* [1980] have shown that arc-like structures are produced by the conical sheet model although no simple choice of parameters has been found which reproduces the data in detail. In particular, the cone emission model does not explain the "nested arcs." These have been attributed to multiple reflections of Alfven waves [*Gurnett and Goertz*, 1981], interference effects [*Boischot and Aubier*, 1981; *Lecacheux et al.*, 1981], and local magnetic anomalies [*Warwick*, 1981].

Hashimoto and Goldstein [1982] used a three-dimensional ray tracing program to investigate the observed occurrence probability maps of the Io-dependent Jovian decametric radiation. They also investigated conditions for wave generation in the Jovian ionosphere. *Goldstein and Theiman* [1981] performed an analytical study of refraction in the Jovian magnetosphere and ionosphere. They demonstrated that an extraordinary wave, initially excited nearly orthogonal to the magnetic field, is significantly influenced by the local plasma density and that arc-like features that resemble those observed are produced by the geometry of the model. In this paper, we extend the work of *Hashimoto and Goldstein* [1983] and *Goldstein and Theiman* [1981] by studying the arc structures using a three-dimensional ray tracing program.

The purpose of this paper is to perform three-dimensional ray tracing of DAM radiation from source positions along an Io flux tube at frequencies greater than but nearly equal to the right-hand extraordinary (RX) mode cutoff frequency $f_{RX} = f_g/2 + ((f_g/2)^2 + f_p^2)^{1/2}$ where f_g is gyrofrequency and f_p is plasma frequency. We have incorporated a realistic Jovian plasma model [*Sentman and Goertz*, 1978], and the O-4 magnetic field model [*Acuna and Ness*, 1976]. Jovian DAM arcs are produced with minimal assumptions about the source mechanism.

RAY TRACING EQUATIONS AND MAGNETOSPHERIC MODEL

Ray Tracing

To calculate propagation ray paths in the Jovian magnetosphere, we have used a three-dimensional ray tracing program. The computer code is based on the *Stix* [1962] cold plasma formulation of the index of refraction and *Haselgrove*'s [1955] set of first order differential equations amenable to numerical solution. The program was initially developed by *Shawhan* [1966] for two-dimensional ray tracing in the terrestial ionosphere and magnetosphere. For the purpose of this three-dimensional ray tracing study, we have incorporated additional equations that allow for variations in the azimuthal direction. This program has been extensively tested and reduces to the two dimensional results of *Green et al.* [1977], *Green and Gurnett* [1980], and *Lecacheaux*

[1] Southwest Research Institute.
[2] NASA Marshall Space Flight Center.
[3] Jet Propulsion Laboratory.
[4] Arecibo Observatory.

Paper number 3A1905.
0148-0227/84/003A-1905$05.00

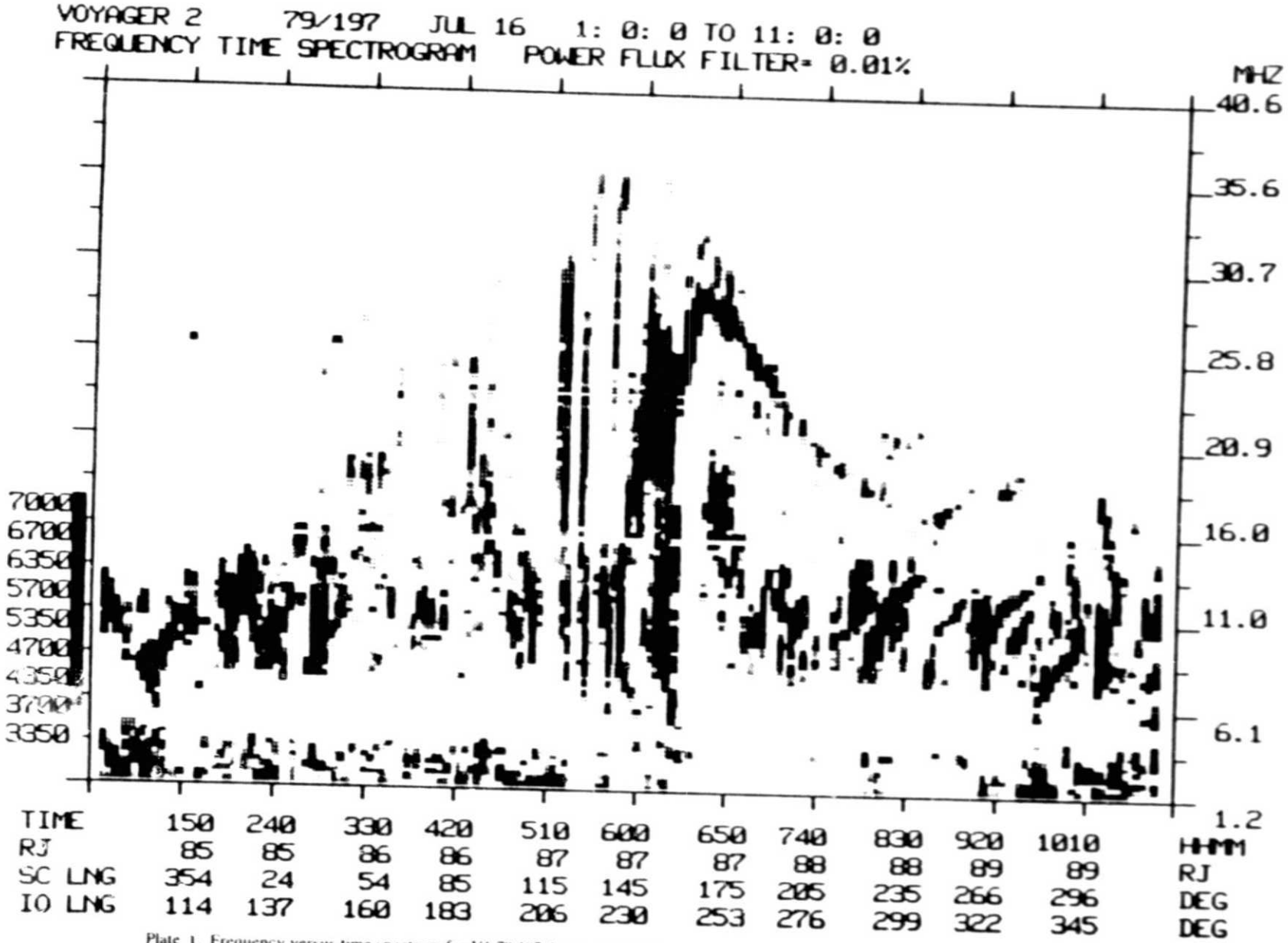

Plate 1. Frequency versus time spectrum for V1-79-197 depicting a series of low curvature nested arcs especially clear between about 510 UT and 600 UT. The "Io LNG" is the Jovian central meridian longitude Io intersects. (The color version and a full description of this figure can be found in the color plate section in this issue.)

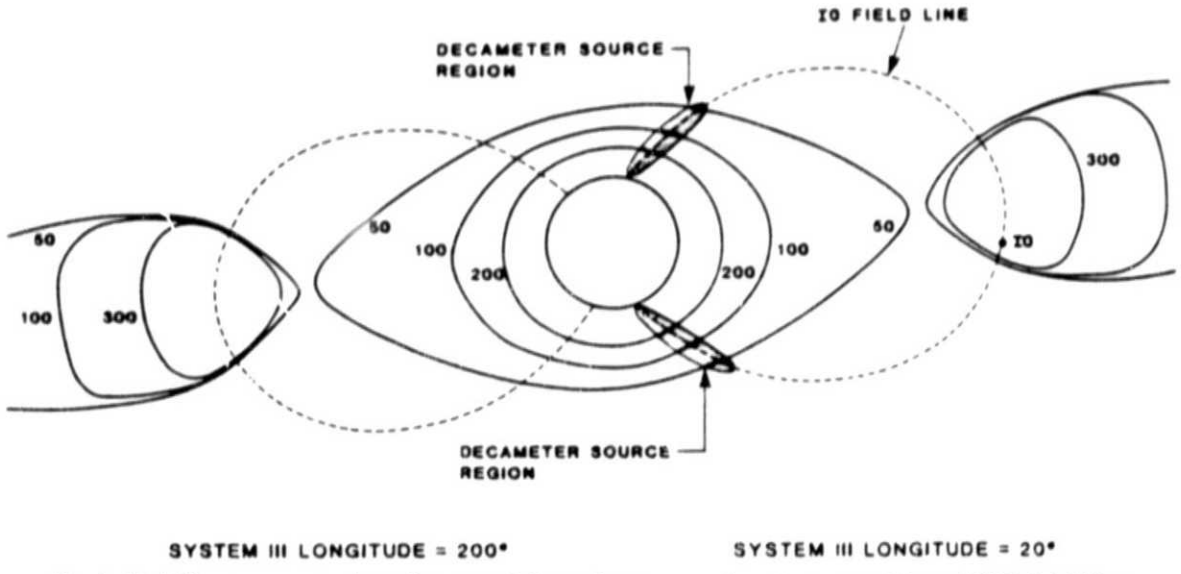

Fig. 1. Model Jovian magnetosphere. Contours of plasma frequency are from *Sentman and Goertz* [1978]. B field from *Acuna and Ness* [1976]. Io torus from *Warwick et al.* [1979].

[1981]. Chosen as inputs are a source position (in radial distance, longitude, and latitude) from which waves at a specific frequency f are to be launched at a specific wave normal angle ψ, with respect to the magnetic field. Different frequencies originating from source points on the same field line or on adjacent field lines would generate a set of nested emission cones. Depending on the geometry of these cones, imposed by the plasma and by the B field, the spacecraft would detect frequencies that decrease or increase with time as these cones sweep over the detector.

At the source region, the program calculates an index of refraction surface for RX mode waves, based on B field and on background plasma parameters. Next, the program takes an incremental step in the direction perpendicular to the index of refraction surface, i.e., in the direction of the group velocity of energy flow, and then determines the coordinates of this new point on the ray path. Then, another index of refraction surface is calculated through this new point and the steps are repeated. The direction of each ray changes according to Snell's law as it travels through the magnetized plasma. To generate an emission cone, thirty-six rays are launched, one every 10° around $\vec{B}$ at the specified wave normal angle and frequency.

B field and Plasma Models

The ray paths calculated by the procedure described above are dependent on the magnetospheric model chosen. The description of the Jovian magnetic field utilized in these calculations (the O-4 model) is that published by *Acuna and Ness* [1976]; the description of the background plasma is that published by *Sentman and Goertz* [1978], and the description the Io torus is that published by *Warwick et al.* [1979]. Figure 1 is an abbreviation of this combined "Jovian magnetosphere" showing contours of plasma frequency in the 200° −20° meridian plane. Suspected source regions in the northern and southern hemispheres are shaded. Spherical harmonic expansion coefficients are used to calculate the magnitude of the field B_0, the components Br, B_θ, and B_ϕ and their derivatives. The plasma density along the ray path, and the spatial gradients are calculated from empirical fits.

As *Hashimoto and Goldstein* [1983] have pointed out, large plasma densities can produce important refractory effects at the higher frequencies when source points near the foot of the Io flux tube extend down into the ionosphere. We have incorporated the ionospheric model introduced by Hashimoto and Goldstein to determine the upper cutoff frequency associated with each Io flux tube investigated in this study, but we have not incorporated an ionospheric model in our ray tracing studies. We have avoided ray tracing at frequencies where ionospheric influence is important. We became aware of the importance of the ionosphere in affecting propagation at certain frequencies only after our extensive ray tracing investigation had almost been completed. Tests at several individual Io flux tubes have indicated that incorporating an ionospheric model that continuously joins with a magnetospheric model will modify our results only slightly at frequencies whose source points lie outside the influence of the ionosphere.

COMPUTATIONS

In addition to the magnetospheric plasma model discussed in the previous section, some assumptions regarding source location, initial launch angle, and mode of propagation are required as inputs to the ray tracing studies. Rather than carrying out a parameter study of these variables, we have chosen a set of initial conditions and studied the propagation over a full range of observer-Io-Jupiter longitude phase space. The results of our studies are intended to show the trends in the radiation spectra introduced by the complex geometry of the problem. Indeed, as we will discuss below,

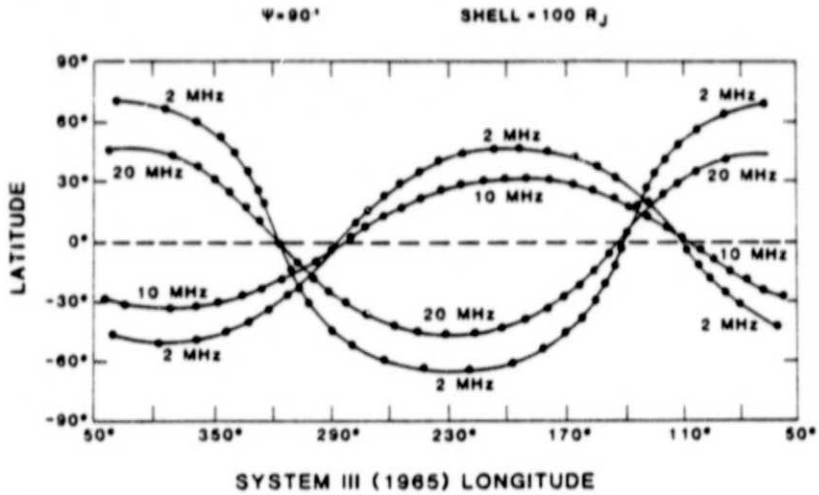

Fig. 2. Calculated radiation sheets for two northern hemisphere sources (2 MHz and 10 MHz) and for two southern hemisphere sources (2 MHz and 20 MHz). The radial shell at 100 Jupiter radii (100 R_J) is shown in mercator projection. All rays were launched at 90° with respect to the B field.

our studies show that exceedingly complex spectra can be produced by propagation effects alone, without introducing complexity into the emission mechanism itself.

The initial conditions we used are as follows:

1. The source region is at the foot of the magnetic L shell that intercepts Io.
2. The frequency of emission in the source region is close to the gyrofrequency and greater than the RX cutoff frequency.
3. The emitted radiation is in the right-hand polarized extraordinary mode.
4. The radiation is emitted in a hollow cone pattern about the magnetic field direction, with the emission angle close to 90° (with respect to the magnetic field).

No specific emission mechanisms are implied by our assumption; rather, they are chosen to be consistent with the available data [i.e., *Carr et al.*, 1983] and to at least some of the theories of radio emissions [i.e., *Dulk*, 1965; *Neubauer*, 1980; *Goertz*, 1980; *Gurnett and Goertz*, 1981; *Goldstein and Goertz*, 1983].

An entire series of ray trajectories are computed for Io positioned every 10° of Jupiter longitude. Typically, Io's position is chosen and a magnetic line of force is calculated from Io to the foot of the flux tube near Jupiter's cloud tops. Source points are located at a set of frequencies, typically 2, 5, 10, 15, 20, 25, 30, and 35 MHz from the condition $f/f_g = 1.005$ at the origin. This latter ratio is chosen to be consistent with slightly Doppler-shifted emission at large wave normal angles. Gyroemission is not assumed. The RX cutoff frequency is calculated and compared with f. Under the condition $f > f_{RX}$, wave propagation is possible and a series of rays is traced at 36 evenly spaced azimuthal directions around the source point. We have also accounted for the oblateness of Jupiter in our determination of f_{RX}. The radial distance to the cloud tops, R(km) is given by $R = 71300(1 - \cos^2(\text{colatitude})/15.4)$. Figure 2 shows on a mercator projection, the intersection of several families of ray trajectories with a sphere of radius 100 R_J that surrounds Jupiter. Shown in the figure are a 2- and 10-MHz family that originate in the northern hemisphere, and a 2- and 20-MHz family that originate in the southern hemisphere.

In all, more than 100 hours of computer time (CPU) on a CYBER 172 was required for the results reported in this study. Typically, 23 min/frequency for each Io position was required to track the ray from the source point out to 150 R_J.

Results

The principal results of our computations are shown in Figures 3*a* and 3*b*. The figure shows the frequencies that would intersect a spacecraft were it located at $R = 150\ R_J$ and at a latitude of 3.2°. The curves are parameterized by the central meridian longitude facing Io at the time of emission. At this distance from the source location, the parallax between the center of the planet and the source is small, and the results apply generally to any observer on this latitude and at a greater distance from Jupiter. The two figures correspond to the two azimuth positions that intersect the observer from every source point (i.e., in general, emission from a cone may intersect the observer in two azimuth directions). The solid curves in Figures 3*a* and 3*b* are not in general what a fixed observer would see because Io is not stationary in the Jovian-fixed longitude system. Hence a stationary observer sees Io moving from longitude to longitude.

Discussion

In Figures 3*a* and 3*b* are revealed the wide range of structure in the curves resulting from varying the Io flux tube longitude of the source points. Indicated by small horizontal brackets on Figures 3*a* and 3*b* are the upper cutoff frequencies for RX mode emission at source point frequencies slightly above the RX cutoff. These cutoffs indicate the maximum frequency that is expected to be emitted along a particular Io flux tube if that emission is slightly above f_{RX}. No DAM emission will escape the ionosphere if the source is at an altitude less than the altitude of the density maximum in the ionosphere. We have so far not performed ray tracing at frequencies that are determined to have sources deep in the ionosphere but have used an ionospheric model only to determine what frequencies will be influenced and the cutoff frequency. Oftentimes, however, one does not observe emission at higher frequencies because those frequencies are

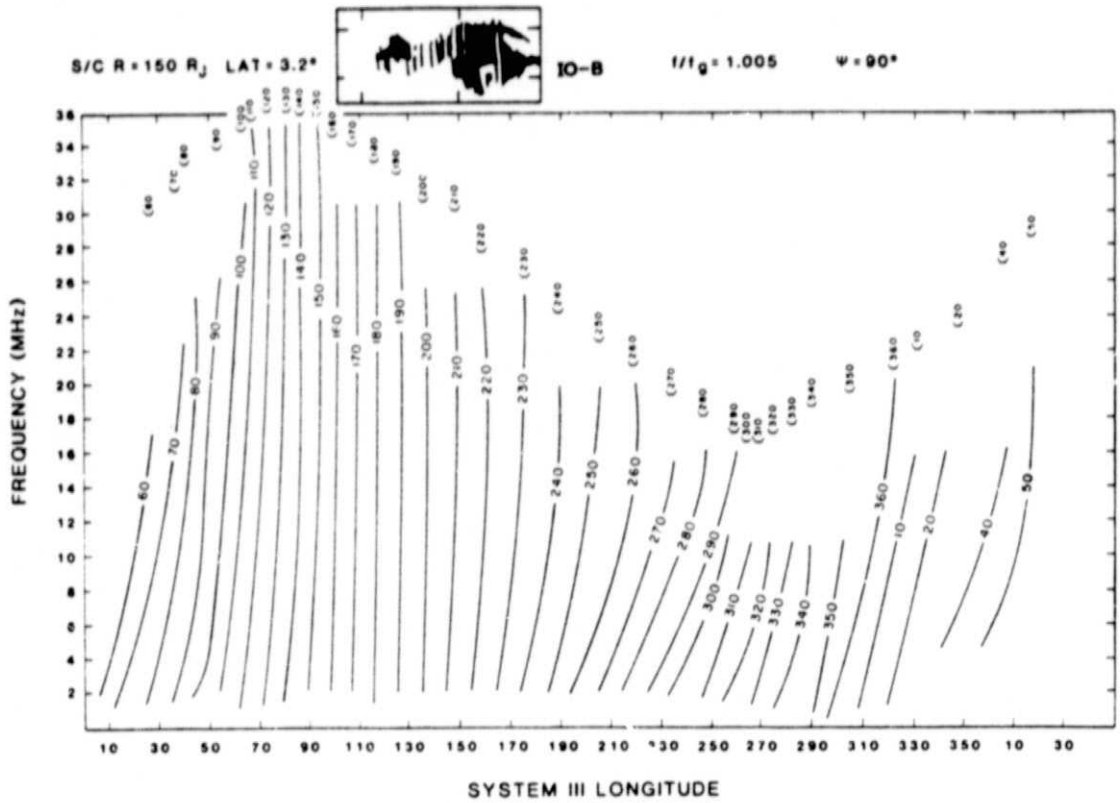

Fig. 3*a*. Frequency versus system III '65 longitude showing the model arcs at 10° intervals of constant Io CML (constant Io format). The Io CML is labeled on each curve. These curves represent the intersection of one "side" of the emission cone with a radial shell at 150 R_J. The horizontal brackets indicate the maximum frequency that can be emitted under the conditions specified in the text. Also indicated are the location of the Io-B source and a modified sketch of part of Figure 7.15 [*Carr et al.*, 1983] indicating the typical signature seen on a dynamic (nonconstant Io) format.

refracted (without ionospheric influence) and do not intercept the spacecraft. The upper cutoff frequency indicated on Figures 3*a* and 3*b* are thus a result of the complex interaction of the magnetic field structure, ionosphere, magnetosphere, and oblateness of Jupiter.

In Figures 3*a* and 3*b* for Io central meridian longitude (CML) in the range from approximately 80° to 240° the curves are rather straight, indicating that multiple frequencies may be observed at a given spacecraft CML. By "Io CML" we mean the sub-Io longitude. For Io CML in the range from 360° through 70° the curves have greater slope, and some show more curvature with a lower but increasing upper cutoff frequency. In the range of Io CML from 250° through 350°, the upper cutoff frequencies are lower with complex structure shown in Figure 3*b* when the spacecraft CML is greater than the CML of Io. It should be noted that while Io may be located at a given CML, the foot of the Io flux tube is not, in general, at the same CML. We believe much of the changing morphology seen in the curves shown in Figures 3*a* and 3*b* is due to the azimuthal asymmetry of the O-4 magnetic field model, which changes the source point field strength and latitude in a circumference of Jupiter.

Also shown superimposed on Figures 3*a* and 3*b* are modified sketches of part of Figure 7.15 from *Carr et al.* [1983]. These sketches indicate the location and typical signatures of the Io-dependent dynamic (non-Io-fixed) spectra. The Io-B source, for instance, generally displays fairly low curvature arcs with smoothly falling upper cutoff frequencies in general agreement with the model arcs of Figure 3*a*. The Io-A source typically displays arcs of more curvature than Io-B source and also displays a lower cutoff frequency with increasing spacecraft CML. The model arcs of Figure 3*b* in the Io-A source region would map to lower curvature arcs on a dynamic (non-Io-fixed) plot, but the upper cutoff frequency does fall off as observed. For the Io-C source the overlap between the observed Io phase and the model Io phase is not as good as for the Io-A and B sources (cf. Table 7.4 of *Carr et al.* [1983]), but the Io-C source region includes both left-hand and right-hand polarization emissions, which indicates possibly some southern hemisphere sources that were not considered in the production of Figure 3. The Io-C source region dynamic spectra show large curvature with rapidly dropping upper cutoff frequency in a region of Figure 3*b* where the model curves show the greatest curvature and a sharp drop in the cutoff frequency.

While the exact arc shape as noted on Figures 3*a* and 3*b* drawn in a constant-Io format should not be directly compared with the dynamic spectra that are drawn in a nonconstant Io format, it is illustrative to note the changes in Io-dependent arc morphology as one moves to the different Io-A, -B, and -C source regions on the constant-Io format on Figures 3*a* and 3*b*. It is tempting to infer that the morphological changes in Io-dependent arc structure as seen on the dynamic spectra can be largely explained by propagation effects rather than by varying emission processes.

Plotting the Voyager PRA data in a constant Io format can be a valuable tool to a better understanding of the emission

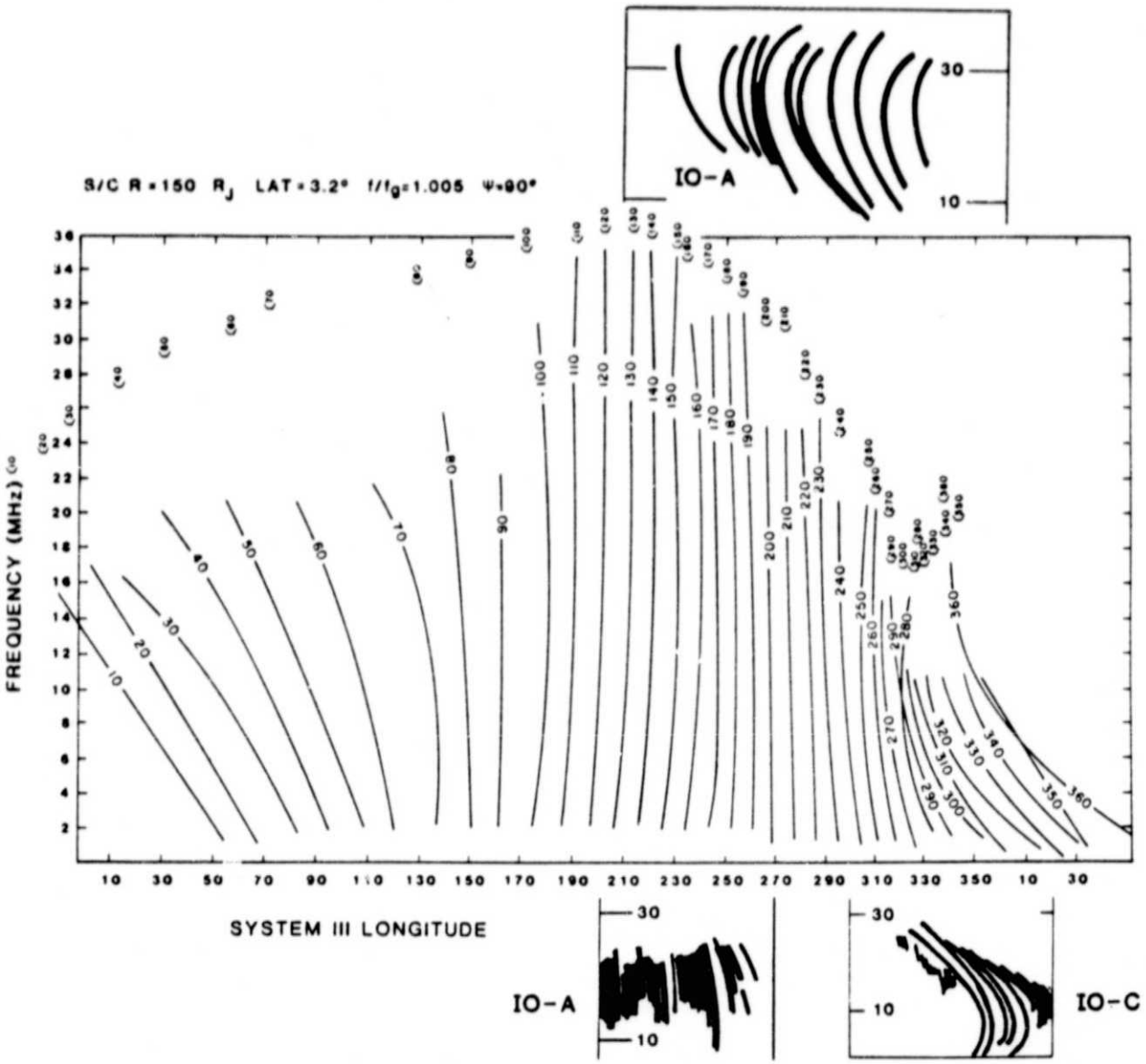

Fig. 3*b*. Same as Figure 3*a* for the other "side" of the emission cone. The Io-A and Io-C source locations and typical dynamic arc signatures are also indicated [*Carr et al.*, 1983].

processes of the Io-dependent sources [cf. *Green*, 1983]. We have avoided replotting Figure 3 in a dynamic-spectra format for direct comparison with the observed Voyager dynamic spectra (although this has been done for specific examples with reasonably good agreement), because we feel the value of Figure 3 is in displaying the major features of Io-dependent emission. The correlation found between Figures 3*a* and 3*b* and the Io-A, -B, and -C source regions supports the initial assumptions pertaining to the emission process, which include RX mode emission almost perpendicular to the magnetic field from source points just above the RX cutoff.

We are currently in the process of comparing reformatted Voyager PRA data with Figure 3 in an effort to understand better the emission process(es) and to explain on a finer scale any differences noted. We recognize these differences may be due to varying wave normal angle [*Goldstein and Thieman*, 1981] and/or discrepancies in the magnetic or plasma field models. In addition, the ionosphere is now known to be of importance at the higher frequencies at some CML values.

Conclusions

We conclude from our results that with minimal assumptions pertaining to an emission mechanism our ray tracing results produce a complex spectrum of Io-dependent DAM arcs as shown in Figures 3*a* and 3*b*. These few assumptions together with the incorporation of the O-4 magnetic field model [*Acuna and Ness*, 1979] and a plasma model due to *Sentman and Goertz* [1978] have resulted in model DAM arcs which display different curvatures and upper cutoff frequencies.

When the source points are located on Io flux tubes that are at Jovian system III longitudes ranging from approximately 90°–230°, where the O-4 model yields high surface magnetic field strengths, Figures 3*a* and 3*b* indicate that the resultant DAM arcs have low curvature and upper cutoff

frequencies extending beyond 35 MHz. On the other hand, when the foot of the Io flux tubes lie in the range of system III longitudes extending from 240°–80°, where the O-4 surface field strengths reach a minimum, the resultant arcs have lower upper cutoff frequency and a higher curvature. It is apparent that the B field structure that produces source points at the foot of the Io flux tube ranging in latitude from 45°–70° and in altitude from 0 to $>2R_J$ around the circumference of Jupiter produces substantial differences in the resultant DAM arcs.

We have also performed preliminary ray tracing studies, including the ionospheric model introduced by *Hashimoto and Goldstein* [1982] and find that the ionosphere can have great influence on emission ray path at the higher frequencies of emission along some Io flux tubes.

Our studies indicate many areas of future attention. We recognize the importance of including the ionosphere in our ray tracing and have begun reproducing our results including an ionosphere for both northern and southern hemisphere sources. In addition, we are investigating the effects of varying the wave normal angle and Doppler shift at the source point. We hope to explain better the higher curvature arcs often observed in the Voyager PRA data.

Because of our apparent success at reproducing, at least qualitatively, some of the Voyager Io-dependent DAM observations, we recognize the importance of reformatting the Voyager PRA data in a manner similar to Figures 3*a* and 3*b*—holding the Io longitude constant [cf. *Green*, 1983].

Acknowledgments. We would like to thank the GSFC radio astronomy group for supplying us with Voyager 1 and 2 PRA data. We would also like to thank Jerome De La Cruz for his assistance in programming. This work was supported by NASA contract NAS7-100 through Cal Tech/JPL contract 956026.

The Editor thanks M. L. Goldstein and C. K. Goertz for their assistance in evaluating this paper.

REFERENCES

Acuna, M. H., and N. F. Ness, The main magnetic field of Jupiter, *J. Geophys. Res.*, *81*, 2917, 1976.

Boischot, A., and M. G. Aubier, The Jovian decametric arcs as an interference pattern, *J. Geophys. Res.*, *86*, 8561, 1981.

Boischot, A., A. Lecacheux, M. L. Kaiser, M. D. Desch, J. K. Alexander, and J. W. Warwick, Radio Jupiter after Voyager: An overview of the planetary radio astronomy observations, *J. Geophys. Res.*, *86*, 8213, 1981.

Carr, T. D., M. D. Desch, and J. K. Alexander, Phenomenology of magnetospheric radio emissions in *Physics of the Jovian Magnetosphere*, edited by A. J. Dessler, p. 226, Cambridge University Press, New York, 1983.

Dulk, G. A., Io-related radio emissions from Jupiter, Ph.D. thesis, Univ. of Colo., Boulder, 1965.

Goertz, C. K., Io's interaction with the plasma torus, *J. Geophys. Res.*, *85*, 2949, 1980.

Goldreich, P., and D. Lynden-Bell, Io, A jovian unipolar inductor, *Astrophys. J.*, *156*, 59, 1969.

Goldstein, M. L., and C. K. Goertz, Theories of radio emissions and plasma waves, in *Physics of the Jovian Magnetosphere*, edited by A. J. Dessler, p. 317, Cambridge University Press, New York, 1983.

Goldstein, M. L., and J. R. Thieman, The formation of arcs in the dynamic spectra of Jovian decametric bursts, *86*, 8569, 1981.

Green, J. L., The Io decametric emission core, *Radio Sci.*, in press, 1984.

Green, J. L., and D. A. Gurnett, Ray tracing of Jovian kilometric radiation, *Geophys. Res. Lett.*, *1*, 65, 1980.

Green, J. L., D. A. Gurnett, and S. D. Shawhan, The angular distribution of auroral kilometric radiation, *J. Geophys. Res.*, *82*, 1825, 1977.

Gurnett, D. A., and C. K. Goertz, Multiple Alfven wave reflections excited by Io: Origin of the Jovian decametric arcs, *J. Geophys. Res.*, *86*, 717, 1981.

Haselgrove, J., Ray theory and a new method of ray tracking, in *Report of Conference on the Physics of the Ionosphere*, pp. 355–364, London Physical Society, London, 1955.

Hashimoto, K., and M. L. Goldstein, A theory of the Io phase asymmetry of the Jovian decametric radiation, *J. Geophys. Res.*, *88*, 2010, 1983.

Leblanc, Y., On the structure of the DAM Jupiter emission, *J. Geophys. Res.*, 8546, 1981.

Lecacheux, A., Ray tracing in the Io plasma torus: Application to the PRA observations during Voyager 1's closest approach, *J. Geophys. Res.*, *86*, 8523, 1981.

Lecacheux, A., N. Meyer-Vernett, and G. Daigne, Jupiter's decametric radio emission: A nice problem of optics, *Astron. Astrophys.*, *94*, L9, 1981.

Neubauer, F. M., Nonlinear standing Alfven wave current system at Io: Theory, *J. Geophys. Res.*, *85*, 1171, 1980.

Pearce, J. B., A heuristic model for Jovian decametric arcs, *J. Geophys. Res.*, *86*, 8579, 1981.

Sentman, D. D., and C. K. Goertz, Whistler mode noise in Jupiter's inner magnetosphere, *J. Geophys. Res.*, *83*, 3151, 1978.

Shawhan, S. D., VLF ray tracing in a model ionosphere, *Res. Rep. 66-33*, Dept. of Phys. and Astron., Univ. of Iowa, Iowa City, 1966.

Smith, R. A., Models of Jovian decametric radiation, *Jupiter*, edited by T. Gehrels, University of Arizona Press, Tucson, 1976.

Staelin, D. H., Character of the Jovian decametric arcs, *J. Geophys. Res.*, *86*, 8581, 1981.

Stix, T. H., *The Theory of Plasma Waves*, pp. 5–34, McGraw-Hill, New York, 1962.

Thieman, R., Jr., and A. G. Smith, Detailed geometric modelling of Jupiter's Io-related decametric radiation, *J. Geophys. Res.*, *84*, 2666, 1979.

Warwick, J. W., Models for Jupiter's decametric arcs, *J. Geophys. Res.*, *86*, 8585, 1981.

Warwick, J. W., J. B. Pearce, A. C. Riddle, J. K. Alexander, M. D. Desch, M. L. Kaiser, J. R. Thieman, T. D. Carr, A. Boischot, C. C. Harvey, and B. M. Pederson, Voyager 1 planetary radio astronomy observations near Jupiter, *Science*, *204*, 995, 1979.

J. L. Green, NASA Marshall Space Flight Center, Huntsville, AL 35812.

S. Gulkis, Jet Propulsion Laboratory, Pasadena, CA 91103.

J. D. Menietti, Southwest Research Institute, P. O. Drawer 28510, San Antonio, TX 78284.

F. Six, Arecibo Observatory, Arecibo, Puerto Rico 00612.

(Received January 31, 1983;
revised October 24, 1983;
accepted November 29, 1983.)

frequencies extending beyond 35 MHz. On the other hand, when the foot of the Io flux tubes lie in the range of system III longitudes extending from 240°–80°, where the O-4 surface field strengths reach a minimum, the resultant arcs have lower upper cutoff frequency and a higher curvature. It is apparent that the B field structure that produces source points at the foot of the Io flux tube ranging in latitude from 45°–70° and in altitude from 0 to $>2R_J$ around the circumference of Jupiter produces substantial differences in the resultant DAM arcs.

We have also performed preliminary ray tracing studies, including the ionospheric model introduced by *Hashimoto and Goldstein* [1982] and find that the ionosphere can have great influence on emission ray path at the higher frequencies of emission along some Io flux tubes.

Our studies indicate many areas of future attention. We recognize the importance of including the ionosphere in our ray tracing and have begun reproducing our results including an ionosphere for both northern and southern hemisphere sources. In addition, we are investigating the effects of varying the wave normal angle and Doppler shift at the source point. We hope to explain better the higher curvature arcs often observed in the Voyager PRA data.

Because of our apparent success at reproducing, at least qualitatively, some of the Voyager Io-dependent DAM observations, we recognize the importance of reformatting the Voyager PRA data in a manner similar to Figures 3*a* and 3*b*—holding the Io longitude constant [cf. *Green*, 1983].

Acknowledgments. We would like to thank the GSFC radio astronomy group for supplying us with Voyager 1 and 2 PRA data. We would also like to thank Jerome De La Cruz for his assistance in programming. This work was supported by NASA contract NAS7-100 through Cal Tech/JPL contract 956026.

The Editor thanks M. L. Goldstein and C. K. Goertz for their assistance in evaluating this paper.

REFERENCES

Acuna, M. H., and N. F. Ness, The main magnetic field of Jupiter, *J. Geophys. Res.*, *81*, 2917, 1976.

Boischot, A., and M. G. Aubier, The Jovian decametric arcs as an interference pattern, *J. Geophys. Res.*, *86*, 8561, 1981.

Boischot, A., A. Lecacheux, M. L. Kaiser, M. D. Desch, J. K. Alexander, and J. W. Warwick, Radio Jupiter after Voyager: An overview of the planetary radio astronomy observations, *J. Geophys. Res.*, *86*, 8213, 1981.

Carr, T. D., M. D. Desch, and J. K. Alexander, Phenomenology of magnetospheric radio emissions in *Physics of the Jovian Magnetosphere*, edited by A. J. Dessler, p. 226, Cambridge University Press, New York, 1983.

Dulk, G. A., Io-related radio emissions from Jupiter, Ph.D. thesis, Univ. of Colo., Boulder, 1965.

Goertz, C. K., Io's interaction with the plasma torus, *J. Geophys. Res.*, *85*, 2949, 1980.

Goldreich, P., and D. Lynden-Bell, Io, A jovian unipolar inductor, *Astrophys. J.*, *156*, 59, 1969.

Goldstein, M. L., and C. K. Goertz, Theories of radio emissions and plasma waves, in *Physics of the Jovian Magnetosphere*, edited by A. J. Dessler, p. 317, Cambridge University Press, New York, 1983.

Goldstein, M. L., and J. R. Thieman, The formation of arcs in the dynamic spectra of Jovian decametric bursts, *86*, 8569, 1981.

Green, J. L., The Io decametric emission core, *Radio Sci.*, in press, 1984.

Green, J. L., and D. A. Gurnett, Ray tracing of Jovian kilometric radiation, *Geophys. Res. Lett.*, *7*, 65, 1980.

Green, J. L., D. A. Gurnett, and S. D. Shawhan, The angular distribution of auroral kilometric radiation, *J. Geophys. Res.*, *82*, 1825, 1977.

Gurnett, D. A., and C. K. Goertz, Multiple Alfven wave reflections excited by Io: Origin of the Jovian decametric arcs, *J. Geophys. Res.*, *86*, 717, 1981.

Haselgrove, J., Ray theory and a new method of ray tracking, in *Report of Conference on the Physics of the Ionosphere*, pp. 355–364, London Physical Society, London, 1955.

Hashimoto, K., and M. L. Goldstein, A theory of the Io phase asymmetry of the Jovian decametric radiation, *J. Geophys. Res.*, *88*, 2010, 1983.

Leblanc, Y., On the structure of the DAM Jupiter emission, *J. Geophys. Res.*, 8546, 1981.

Lecacheux, A., Ray tracing in the Io plasma torus: Application to the PRA observations during Voyager 1's closest approach, *J. Geophys. Res.*, *86*, 8523, 1981.

Lecacheux, A., N. Meyer-Vernett, and G. Daigne, Jupiter's decametric radio emission: A nice problem of optics, *Astron. Astrophys.*, *94*, L9, 1981.

Neubauer, F. M., Nonlinear standing Alfven wave current system at Io: Theory, *J. Geophys. Res.*, *85*, 1171, 1980.

Pearce, J. B., A heuristic model for Jovian decametric arcs, *J. Geophys. Res.*, *86*, 8579, 1981.

Sentman, D. D., and C. K. Goertz, Whistler mode noise in Jupiter's inner magnetosphere, *J. Geophys. Res.*, *83*, 3151, 1978.

Shawhan, S. D., VLF ray tracing in a model ionosphere, *Res. Rep. 66-33*, Dept. of Phys. and Astron., Univ. of Iowa, Iowa City, 1966.

Smith, R. A., Models of Jovian decametric radiation, *Jupiter*, edited by T. Gehrels, University of Arizona Press, Tucson, 1976.

Staelin, D. H., Character of the Jovian decametric arcs, *J. Geophys. Res.*, *86*, 8581, 1981.

Stix, T. H., *The Theory of Plasma Waves*, pp. 5–34, McGraw-Hill, New York, 1962.

Thieman, R., Jr., and A. G. Smith, Detailed geometric modelling of Jupiter's Io-related decametric radiation, *J. Geophys. Res.*, *84*, 2666, 1979.

Warwick, J. W., Models for Jupiter's decametric arcs, *J. Geophys. Res.*, *86*, 8585, 1981.

Warwick, J. W., J. B. Pearce, A. C. Riddle, J. K. Alexander, M. D. Desch, M. L. Kaiser, J. R. Thieman, T. D. Carr, A. Boischot, C. C. Harvey, and B. M. Pederson, Voyager 1 planetary radio astronomy observations near Jupiter, *Science*, *204*, 995, 1979.

J. L. Green, NASA Marshall Space Flight Center, Huntsville, AL 35812.

S. Gulkis, Jet Propulsion Laboratory, Pasadena, CA 91103.

J. D. Menietti, Southwest Research Institute, P. O. Drawer 28510, San Antonio, TX 78284.

F. Six, Arecibo Observatory, Arecibo, Puerto Rico 00612.

(Received January 31, 1983;
revised October 24, 1983;
accepted November 29, 1983.)

B. Appendix 2: "Identification of Decametric Radiation from Sources in the Southern Hemisphere in Jupiter"

IDENTIFICATION OF DECAMETRIC RADIATION FROM THE SOUTHERN HEMISPHERE OF JUPITER

by

J. Douglas Menietti
Southwest Research Institute
San Antonio, Texas 78284

James L. Green
Space Science Laboratory
NASA Marshall Space Flight Center
Huntsville, Alabama 35812

April 1984

Submitted to Journal of Geophysical Research

ABSTRACT

A technique has been developed which aids the identification of Io-dependent decametric radiation originating from the southern hemisphere of Jupiter. This technique compares the results of model ray tracing calculations with the Planetary Radio Astronomy (PRA) observations. All Voyager 1 or 2 PRA observations are sorted into bins (±3° wide) centered on a specific Io cental meridian longitude. When the data is plotted (as a frequency-longitude spectrogram) in this coordinate system, Io-dependent features can be identified and used for direct comparison with model ray tracing calculations. The ray tracing calculations are done in a model Jovian magnetosphere where it is assumed that the decametric emissions are generated in the RX mode from low altitude source regions along the instantaneous Io flux tube. In this study, we compare the observations taken for four specific Io longitudes (150°, 160°, 170°, and 260°) with the corresponding model ray tracing. The Voyager observations and the model ray tracing calculations, when combined, clearly distinguish the northern and southern hemisphere emission features. This method allows, for the first time, Io-dependent DAM emissions generated in the southern and northern hemisphere to be delineated.

INTRODUCTION

The complete spectrum of Jovian decametric (DAM) radiation was first observed by the Voyager Planetary Radio Astronomy (PRA) experiment (Warwick et al., 1979). One of the most striking features of the Jovian DAM emissions seen in frequency-time spectrograms, are "arc-like" bands. The frequency range of the arc emissions is from 1 to almost 40 MHz, but not all arcs span this complete frequency range. Several different types of arcs have been recognized in the data, depending on their curvatures which either open toward increasing time (vertex early) or open toward decreasing time (vertex late). In general, an arc may appear either as an isolated feature or there may be a series of closely spaced arcs (called "nested arcs"). Detailed descriptions of the Jovian decametric arcs can be found elsewhere (ie., Warwick et al., 1979; Leblanc, 1981; Boischot and Aubier, 1981; Carr, Desch, and Alexander, 1983).

A general feature of most propagation theories of the DAM arc producing mechanism is that the emission occurs along conical sheets that are swept past the observer as the planet rotates as first suggested by Dulk (1967). Many investigators attribute the emission to precipitating electrons along the Io magnetic flux tube which radiate near the gyrofrequency (Goldreich and Lynden-Bell (1969); Smith (1976); Goldstein and Goertz, 1983). Goldstein and Thieman (1981); Pearce (1981); Staelin (1981); Neubauer, (1980) have shown that arc-like structures are produced by a conical sheet model although no simple choice of parameters has been found which reproduces the data in detail. In particular, these simple emission cone models do not explain the "nested arcs". However, nested arcs have been attributed to multiple reflections of Alfven waves (Gurnett and Goertz, 1981), interference effects (Boischot and Aubier, 1981; Lecacheux, 1981), and local magnetic anomalies

(Warwick, 1981). As shown by Goldstein and Thieman (1981) and Menietti et al. (1984), the arc curvature which varies on a frequency-time spectrogram from almost zero to quite dramatic loops (great arcs) may result from variations of the wave normal angle as a function of frequency in the source region. Hashimoto and Goldstein (1983) have suggested that the Io phase asymmetry of the DAM arcs may be due to the difference in propagation time of Alfven waves reflected from both the northern and southern hemisphere Jovian ionosphere.

The purpose of this paper is to compare three-dimensional ray tracing of Jovian DAM emissions, from the southern and northern hemisphere, with the PRA measurements in order to determine the frequency-time signatures of southern hemisphere arcs. This paper complements the northern hemisphere ray tracing of Menietti et. al. (1984). The observations will be transformed into an Io-Jupiter stationary coordinate system (see Green, 1984). This coordinate system allows for the Io-dependent emission features observed by the PRA experiment to be directly compared with the model ray tracing results. We have chosen source regions at four sub-Io longitudes. The agreement between the Voyager observations and the model ray tracing is good and allows the separation of the northern and southern hemisphere emission features. With this technique the southern and northern hemisphere decametric sources have, we believe, for the first time been delineated. The good agreement between the observations and the ray tracing results provides strong evidence that the basic assumptions of the model are correct. Refinements are necessary, however, to reproduce exact details of the emissions.

THE RAY TRACING PROGRAM

The ray tracing program used for this study is discussed in some detail in Menietti et al. (1984). Briefly, the Jovian magnetosphere used is the O-4 magnetic field model of Acuna and Ness (1976), and the Jovian background magnetospheric plasma is given by the model proposed by Sentman and Goertz (1979). The Io torus plasma density is a spline fit to the published contours of Warwick et al. (1979). In addition, the computer code contains an empirical model of the Jovian ionosphere based on the results of Hashimoto and Goldstein (1983). The program is based on a closed set of first order differential equations in spherical polar coordinates specialized by Shawhan (1966) (in two dimensions) and by Menietti et al. (1984) (in three dimensions) that describe the path of rays in a magnetized plasma. The expressions for the phase index of refraction and its derivatives are in the cold plasma formulation of Stix (1962).

Qualitatively, the program calculates an index of refraction surface and group velocity (magnitude and direction) for a predetermined plasma wave mode in the model magnetosphere at some starting point. The program then takes an incremental step in the direction of the group velocity or energy flow and determines the coordinates of a new point on the raypath. Another index of refraction surface is calculated at this new point and the steps are repeated. The program used here has been extensively tested and reduces to the two-dimensional results of Green and Gurnett (1980) and Lecacheux (1981).

MODEL ASSUMPTIONS

The following assumptions regarding source location, initial launch angle and mode of propagation are required as inputs to the ray tracing program:

1. The source region is at the foot of the magnetic L-shell which intercepts Io;
2. The frequency of emission in the source region is close to the gyrofrequency and greater than the RX cutoff frequency;
3. The emitted radiation is in the right-hand polarized extraordinary mode; and
4. The radiation is emitted in a hollow cone pattern about the magnetic field direction. The emission angle with respect to the magnetic field was set equal to 85° for northern hemisphere sources and to both 85° and 95° for southern hemisphere sources.

No specific emission mechanisms are implied by our assumptions; rather, they are chosen to be consistent with the available data (i.e. Carr et al., 1983) and at least some of the theories of radio emissions (i.e. Dulk, 1967; Neubauer, 1980, Goertz, 1980; Gurnett and Goertz, 1981; Goldstein and Goertz, 1983).

We have computed ray trajectories for sources located at sub-Io longitudes located every 10° of Jovian longitude, for both northern and southern hemisphere sources. Source points are located along an Io flux tube at a set of frequencies, typically 2, 5, 10, 15, 20, 25, 30, and 35 MHz from the condition $f/f_g=1.01$ at the the origin. This latter ratio is chosen to be consistent with slightly Doppler-shifted emission at a wave normal angle, Ψ_o, of 85° (cf. Staelin, 1981). Gyroemission is not assumed. Under the condition that the wave frequency is greater than the RX cutoff frequency, wave propagation is possible and a series of rays, for a constant frequency, is traced at 36 evenly spaced azimuthal directions around the magnetic field at the chosen source location. In the determination of the location of the RX

cutoff frequency, the oblateness of Jupiter is accounted for; the radial distance to the cloud tops is given by R = 71300 (1-cos^2(colatitude)/15.4). The intersection of the resulting generated emission cones, for all frequencies, at 150 R_J and at a latitude of 5° determines the model decametric emission spectrum. It is this model decametric spectrum which is compared with the observations. For the purposes of this study we have chosen only four sub-Io longitudes to compare directly with observations which we feel clearly depict those emissions from southern hemisphere sources.

COMPARISON OF OBSERVATIONS AND RAY TRACING RESULTS

Only PRA observations made from February 21 to March 18, 1979 by Voyager 1 and from June 26 to July 23, 1979 by Voyager 2 are used in this study. These observations are approximately centered around the encounter period and comprise enough data for a complete frequency-longitude study of Io-dependent DAM emissions to be made. Observations at radial distances of less than 30 R_J were excluded in order to avoid the changing emission pattern due to inner-magnetospheric propagation effects. The frequency-longitude spectrogram for Voyager 1 and 2 data (sub-Io system-III longitude of 260°) is shown in Figure 1. This figure displays Voyager 1 and 2 data transformed into a coordinate system where the sub-Io system-III longitude was equal to 260° (±3°) The data displayed in Figure 1 is only a subset of the entire Voyager data. It is important to note that a band of emission extending in frequency from about 6 to 13 MHz seen at all Jovian system-III longitudes in Figure 1 (as well as in Figures 2-4) is partially due to an increase in the sensitivity of the PRA instrument at these frequencies (Schauble and Carr, 1983).

Clearly seen in Figure 1 are two rather narrow emission zones. One located at Jovian system-III longitudes between approximately 155°-185° and

another located between about 305°-330°. Both of these emission zones extend to over 30 MHz. In the region between these two narrow emission zones which will hereafter be referred to as northern hemisphere emissions (NHE) is a region of less distinct but nevertheless structured emission which extends between about 215°-305° and in frequency from about 5-25 MHz. There is a narrow emission feature centered at about 60° and extending in frequency to possibly over 30 MHz but careful examination of this feature reveals that it is due to spacecraft noise (interference from other instruments). In addition, the emissions seen centered around 140° and extending to about 26 MHz, and the emissions at about 274° and extending in frequency to almost 40 MHz, are also of spacecraft origin.

Also shown on Figures 1-4 are the results of ray tracing emission from both northern (circles) and southern (triangles and squares) hemisphere sources. The ray tracing results for the southern hemisphere sources are shown for initial wave normal angles of 95° (triangles) and 85° (squares) in order to investigate the dependence of the resulting arcs on this parameter. The agreement for the northern hemisphere emissions is relatively good with respect to Jovian longitude. Seen in Figure 1 are model emissions within Jovian longitude range 180°-186° and emissions at about 335°. Both of the model northern emission cone edges are quite narrow in longitude extent. These northern hemisphere model emission cones lie close to the range of the observed northern emission cones shown in the same figure, but shifted possibility 10° to higher longitudes. The frequency extent for the model emission cones is less than observed, however, by about 15 MHz. The reason for this discrepancy may to be due to inadequacies in the magnetic field model. An increase in the magnetic field strength at the source point from about 7 gauss to over 10 gauss would be required for emission at 30 MHz to be

allowed. This large increase in the field strength suggests either errors in the model at low altitudes or transient effects. Since Figure 1 represents data taken over a long period of time by two satellites it is possible that the observed emissions at the highest frequencies are temporal effects of the nonquiescent Jovian magnetic field.

The model southern emission cones are also shown at specific frequencies on Figure 1 superimposed as triangles and squares for clarity. While the agreement is not perfect, it is clear that the emissions between the northern emission cones shown in Figure 1 are southern hemisphere emissions. The frequency extent is less than that of the NHE and the characteristic "arch-shape" is easily discernable. The "left" edge of the arch formed by the observed emission from the southern hemisphere is bracketed by the model emissions for wave normal angles of 95° and 85°. The "right" edge of the model emission cone is displaced from the observed right edge of the "arch" by possibly 30° or so. Changing the initial wave normal angle could produce a match with the observations, but so would the introduction of a magnetic field model with a different azimuthal dependence.

Figure 2 is the same format as Figure 1 but now for a fixed sub-Io longitude of 160°. In this figure the two observed NHE zones are between about 40°-90° longitude and between about 195°-240°. The NHE zones are not as distinct as they are in Figure 1. There are, for example, reasonably intense emissions in the longitude range of 40°-70° and in the frequency range of about 17-20 MHz. Another emission region appears to be located in the longitude range of about 195°-230° and frequency range 16-23 MHz. These emissions broaden the NHE zones and may represent statistical variations of

the NHE zones or they may represent emissions not modelled by the present assumptions. The results of the ray tracing are shown on Figure 2 as circles for the model NHE zones. The model fit is good, but it is apparent that the observed "right" NHE zone (at about 235°) is smaller in frequency extent than the observed "left" NHE zone (at about 80°), and smaller in frequency extent than the model NHE zone. This phenomena, one side of the emission cone having a smaller frequency extent than the other, is observed frequently in the data and is thus far not adequately modelled. One possible explanation is the refractive effects of the Jovian ionosphere which, because of geometry, are more extensive on one of the emission cones. This effect is currently being investigated. The emissions between the observed NHE cones are not as structured as in the example of Figure 1, but it is clear that intense radiation persists close to the emission cones produced by the model ray tracing and shown as the triangles and circles on Figure 2. While not perfect, the qualitative agreement leaves little doubt that the emissions between the NHE zones are from the southern hemisphere. For this example the right edge of the emission cone is more distinct and appears to be bracketed by the model ray tracing results for the two initial wave normal angles.

The sorted Voyager data shown in Figure 3 is for sub-Io longitude of 170°. For this example the southern hemisphere emission (SHE) occurs between about 95°-210° at frequencies less than 25 MHz and has the characteristic "arch-shape" described above. The ray tracing results match the SHE very nicely, with the "right" edge of the emission cone agreeing better with the model for Ψ_o=85°. The NHE zones are broad and not distinct. The "right" NHE zone extends from about 190° to about 310° with a peak frequency occurring between 245°-265°. The model ray tracing results fall close to the center of this range around 260°. The "left" edge of the observed NHE zone is also not

very distinct, but appears to be between 35°-80° longitude, with a frequency peak possibly between 50°-80°. The model ray tracing results for the "left" edge of the NHE zone appear to be shifted by about 15° to 20° to the right (higher longitudes) from the observed NHE zone. The data for this sub-Io longitude contains a great deal of s/c noise which confuses the match with the NHE zones. We have chosen Figure 3 with the confusion of emissions and noise to point out the distinctive southern hemisphere emissions.

The sorted data for sub-Io longitude 150° is shown in Figure 4. The most distinctive feature is the band of emission extending in frequency from about 20 MHz to about 5 MHz and extending in longitude from about 160° to about 220°. This is identified as the "right" edge of the SHE emission and the model ray tracing results bracket this feature reasonably well. The "left" edge of the SHE is not as distinct and may overlap with the NHE zone at about 75°. The observed NHE zones are not clearly defined. The "left" zone may extend from about 35° to almost 100°, and in frequency to over 35 MHz. The other NHE zone is even less well defined but may extend from about 200° to over 300° with a strong feature at 252°, but emission over 25 MHz is not well defined. The model ray tracing results for the NHE at about 75° and at about 235° are within the observed regions of NHE, but the ray tracing results extend to 35 MHz. We have included this figure also to demonstrate the distinctive SHE emission even though the NHE zones are much less discrete.

DISCUSSION

To our knowledge the results presented here represent the first identification of Jovian southern hemisphere DAM emissions. This identification has been made possible not only by the comprehensive

three-dimensional ray tracing utilizing realistic magnetospheric and ionospheric plasma and magnetic field models, but also the sorting of the Voyager data set with respect to constant sub-Io longitudes. This has allowed the quick analysis of many months of Voyager data in a reference frame best adapted for study of Io-dependent DAM emissions. The southern hemisphere DAM emissions observed are in general lower in frequency and the emission cones are narrower. The first of these observations can be explained by noting that the southern hemisphere emission sources occur on weaker magnetic field lines than northern sources (cf. Acuna and Ness, 1976), and the emission is restricted to be slightly Doppler-shifted above the RX cutoff frequency. A narrower emission cone results because the Voyager spacecraft, being confined approximately to the ecliptic plane, intersects the emission cones from the northern hemisphere sources closer to the central radius. In other words, the emission cones of the southern hemisphere sources are often inside the NHE cones. Since the magnetic field is weaker in the southern hemisphere, the ratio, f_p/f_g, will be larger for the same source frequency resulting in additional refraction and a smaller emission cone angle. The latter fact also explains the "arch-shape" or tendency for the highest frequency emission to occur at the same Jovian longitude which appears frequently among the southern hemisphere sources. For consecutive frequencies the SHE cones will be confined to a smaller range of longitudes than the corresponding NHE cones at consecutive frequencies, and the net effect is to produce a bunching of the higher frequency ray paths.

SUMMARY

We have presented a comparison of the results of three-dimensional ray tracing of Jovian DAM emissions from both southern and northern hemisphere source positions. The ray tracing is based on a minimum number of assumptions which include RX mode emission from source points slightly Doppler-shifted above the RX cutoff. A constant initial wave normal angle of 85° was assumed for the northern hemisphere sources and both 85° and 95° for the southern hemisphere sources, consistent with the results of Staelin, 1981 for electrons with energies of several keV. The plasma model is an empirical fit which includes the effects of the ionosphere, Io torus, and magnetosphere. The magnetic field is the O-4 model (Acuna and Ness, 1976). The Voyager 1 and 2 data have been sorted to hold the sub-Io longitude constant in order to clearly display the Io-dependent features. When directly compared to the sorted Voyager data, the ray tracing results clearly distinguish the northern and southern emission features. It is found that the southern Io-dependent DAM emissions are, in general, lower in frequency, and the emission cone edges are observed closer together in longitude along the spacecraft trajectory as expected from the model.

This study shows that the identification of southern hemisphere DAM emission establishes strong support that Jovian DAM emission features observed by the PRA experiment are primarily due to propagation effects. A simple model of wave propagation at large wave normal angles from sources along the Io flux tube agrees quite well with many of the Voyager observations. There are, of course, discrepancies that need to be addressed such as the observed higher upper frequency cutoff of the NHE on Figure 1, for example. In addition, there are other interesting Io-dependent features observed such as

emission observed at the sub-Io longitude of observation (the current Io flux tube). We are aware of the power of sorting the data in displaying what would otherwise be subtle features in the data set. Attempts to model specific arc features can be very frustrating on an individual basis, and the sorting technique allows rapid display of qualitative features. We are currently introducing new plasma and magnetic field models in an effort to improve the model and we will be examining other frequency ranges by the same procedure.

ACKNOWLEDGEMENTS

The authors are grateful to Dr. James Warwick and the Planetary Radio Astronomy team (in particular M. Kaiser) for the use of the Voyager 1 and 2 time-averaged PRA calibrated data. Helpful discussions with Drs. N. F. Six and S. Gulkis are gratefully acknowledged. This research was supported by the National Aeronautics and Space Administration under the Jupiter Data Analysis Program, through NASA contract NAS7-100 and through Cal Tech/JPL contract 956026. The authors would also like to express their gratitude to the Data System Technology Program for allowing access to the central computer facilities and to the Space plasma Computer Analysis Network (SCAN).

REFERENCES

Acuna M. H., and N. F. Ness, "The main magnetic field of Jupiter", J. Geophys. Res., 81, 2917, 1976.

Boischot, A. and M. G. Aubier, "The Jovian Decametric Arcs As An Interference Pattern", J. Geophys. Res., 86, 8561, 1981.

Carr, T. D., M. D. Desch, and J. K. Alexander, "Phenomenology of Magnetospheric Radio Emission", in Physics of the Jovian Magnetosphere, A. J. Dessler (Editor), Cambridge University Press, New York, 1983.

Dulk, G. A., "Apparent Changes in the Rotation Rate of Jupiter", Icarus, 7, 173, 1967.

Goertz, C. K., "Io's Interaction With the Plasma Torus", J. Geophys. Res., 85, 2949, 1980.

Goldreich, P. and D. Lynden-Bell, "Io, A Jovian Unipolar Inductor", Astrophys. J., 156, 59, 1969.

Goldstein, M. L., and J. R. Thieman, "The Formation of Arcs in the Dynamic Spectra of Jovian Decametric Bursts", J. Geophys. Res., 86, 8568, 1981.

Goldstein, M. L., and C. K. Goertz, "Theories of Radio Emissions and Plasma Waves", in Physics of the Jovian Magnetosphere, A. J. Dessler (Editor), Cambridge University Press, New York, 1983.

Green, J. L., and D. A. Gurnett, "Ray Tracing of Jovian Kilometric Radiation", Geophys. Res. Lett., 7, 65, 1980.

Green, J. L., "The Io Decametric Emission Cone", Radio Science, 19, 556, 1984.

Gurnett, D. A., and C. K. Goertz, "Multiple Alfven Wave Relections Excited by Io: Origin of the Jovian Decametric Arcs", J. Geophys. Res., 86, 717, 1981.

Hashimoto, Kozo and Melvyn L. Goldstein, "A Theory of the Io Phase Asymmetry of the Jovian Decametric Radiation", J. Geophys. Res., 88, 2010, 1983.

Leblanc, Y., "On the Arc Structure of the DAM Jupiter Emission", J. Geophys. Res., 86, 8564, 1981.

Lecacheux, Alain, "Ray Tracing in the Io Plasma Torus: Application to the PRA Observations During Voyager 1's Closest Approach", J. Geophys. Res., 86, 8523, 1981.

Menietti, J. D., J. L. Green, S. Gulkis, F. N. Six, "Three Dimensional Ray Tracing of the Jovian Magnetosphere in the Low Frequency Range", J. Geophys. Res., 89, 1489, 1984.

Neubauer, F. M., "Nonlinear Standing Alfven Wave Current System at Io: Theory", J. Geophys. Res., 85, 1171, 1980.

Pearce, J. B., "A Heuristic Model for Jovian Decametric Arcs", J. Geophys. Res., 86, 8579, 1981.

Schauble, John J. and Thomas D. Carr, "Calibration of the Voyager Planetary Radio Astronomy Radiometers Above 4 MHz", Paper presented at the National Radio Science Meeting, Boulder, Colorado, January 6, 1983.

Shawhan, S. D., "VLF Ray Tracing in a Model Ionosphere" Dept. of Physics and Astronomy, U of Iowa Res. Rept. 66-33, 1966.

Sentman D. D., and C. K. Goertz, "Whistler Mode Noise in Jupiter's Inner Magnetosphere", J. Geophys. Res., 83, 3151, 1978.

Smith, R. A., "Models of Jovian Decametric Radiation", Jupiter, edited by T. Gehrels, University of Arizona Press, Tucson, 1976.

Staelin, D. H., "Character of the Jovian Decametric Arcs", J. Geophys. Res., 86, 8581, 1981.

Stix, T. H., The Theory of Plasma Waves, McGraw-Hill Book Co. Inc., 1962.

Warwick, J. W., J. B. Pearce, A. C. Riddle, J. K. Alexander, M. D. Desch, M. L. Kaiser, J. R. Thieman, T. D. Carr, S. Gulkis, A. Boischot, C. C. Harvey, and B. M. Pedersen, "Voyager 1 Planetary Radio Astronomy Observations Near Jupiter", Science, 204, 995, 1979.

Warwick, J. W., "Models for Jupiter's Decametric Arcs", J. Geophys. Res., 86, 8585, 1981.

FIGURE CAPTIONS

Figure 1. Voyager 1 PRA high-band (1.2 to 40.6 MHz) data (from February 21 to March 18, 1979) and Voyager 2 PRA high-band data from (June 26 to July 23, 1979) have been placed in bins of spacecraft system III longitude (1965) when Io is within ±3° around 260° system III longitude. Superimposed on the Voyager data are the model ray tracing results for source points in the northern hemisphere (blue circles; Ψ_o=85°) and for source points in the southern hemisphere (green triangles [Ψ_o=95°] and red squares [Ψ_o=85°]). Note the narrow "arch" of emission between longitudes of about 200° and 300° which we believe is due to southern hemisphere sources.

Figure 2. The format is the same as Figure 1 but now Io is within ±3° around 160° system III longitude. In this figure the "arch" of emission is not as distinct as in Figure 1 but there is a "ramp" of emission corresponding to one edge of the southern hemisphere emission cone which is bracketed by the model ray tracing results between longitudes about 150° and 200°.

Figure 3. The format is the same as Figure 1 but with Io centered around 170° system III longitude. While much of s/c instrument interference is present in this figure, the southern hemisphere emission is reasonably distinct in its characteristic "arch" between longitudes of about 100° and 200° and bracketed by the model ray tracing results.

Figure 4. The format is the same as Figure 1 but with Io centered around 150° system III longitude. Only one edge of the southern hemisphere emission cone is distinct between longitudes about 150° to about 200° and bracketed by the model ray tracing results.

C. Appendix 3: "Jovian Decametric Arcs: An Estimate of the Required Wave Normal Angles from Three-Dimensional Ray Tracing"

JOVIAN DECAMETRIC ARCS: AN ESTIMATE OF THE REQUIRED WAVE NORMAL ANGLES FROM THREE-DIMENSIONAL RAY TRACING

J. D. Menietti[1], J. L. Green[2], S. Gulkis[3] and N. F. Six[4]

[1]Southwest Research Institute, Post Office Drawer 28510, San Antonio, TX 78284

[2]Marshall Space Flight Center, Huntsville, AL 35812

[3]Jet Propulsion Laboratory, Pasadena CA 91103

[4]Arecibo Observatory, Arecibo, Puerto Rico

Abstract. A three-dimensional ray tracing code which incorporates the O-4 magnetic field model (Acuna and Ness, 1979) and a realistic plasma model has been used to model high-curvature decametric arcs observed by the Voyager Planetary Radio Astronomy (PRA) instrument. Two examples of intense, isolated, vertex-late, high-curvature arcs were singled out for study. The source point wave normal angle was incremented at each of a full range of frequencies until the model rays identically matched the observed arcs of the PRA data. Several different Doppler shifts were assumed at the source point. By this procedure, an accurate relationship between the wave normal angle, Ψ, and the frequency was obtained, with the variation being $70° < \Psi < 80°$, and $\Psi_{MAX}=80°$ for the arcs considered. As the assumed Doppler shift at the source point increased, the value of Ψ_{MAX} was found to decrease, but the general shape of the $\Psi(f)$ curve was unaffected. By comparing the ray tracing results with the independent results of Staelin (1981) regarding emission from beaming electrons, it was found that larger Doppler shifts ($f/f_g > 1.1$) at the source point produce $\Psi_{MAX} > 70°$, in agreement with the ray tracing results for the two arcs considered, only for $v_\parallel > 0.7$ and $v_\parallel/c > 0.32$ (where $v_\parallel$ = electron velocity parallel to $\overline{B}$). Actual values of $v_\parallel/v$ are unknown, but independent observations indicate that $v_\parallel/c \approx 0.1$. Since the low-curvature arcs are believed to result from larger wave normal angles, our results indicate an upper limit to the Doppler shift, of Jovian DAM emissions of $f/fg < 1.1$.

Introduction

Frequency-time spectrograms of the Voyager I and II low-frequency (1 MHz to 40 MHz) observations clearly reveal Decametric (DAM) "arc" signatures with various radii of curvature (Boischot, 1981; Lecacheux, 1981). In the top panel of Figure 1 are displayed DAM arcs observed by Voyager 1 on day 197 of 1979. The low-curvature arcs seen from about 0510 UT to 0550 UT represent one class of event while high-curvature arcs seem to represent a different class. A typical example of a high-curvature arc observed by Voyager 1 on day 72 of 1979 is displayed in the lower panel of Figure 1, extending at both high and low frequencies from about 1150 UT to the arc vertex at about 1235 UT. Several authors have performed ray tracing analyses utilizing model Jovian magnetospheres in order to reproduce the DAM arc features [Goldstein and Thieman (1981), Menietti et al. (1984), Green (1984)]. These initial efforts displayed some success in reproducing the characteristic arc shape with a minimum number of assumptions about the emission mechanism. Goldstein and Thieman (1981) have found, using an elementary ray tracing analysis, that varying the wave normal angle was essential to accurately compare model-generated to observed DAM arcs. Goldstein and Thieman obtained an empirical relationship to describe the dependence of wave normal angle, Ψ, on emission frequency, f. Their results indicated that Ψ is not a linear function of f but rather has a variable peak at a mid-range frequency. These results were based on a two-dimensional ray tracing code and represent an initial analysis. Hashimoto and Goldstein (1983) published the first three-dimensional Jovian ray tracing results which offered a convincing explanation of the DAM assymmetry of the source position relative to the central meridian longitude of Io. A major contribution of their work was in pointing out the significance of the ionosphere in refracting DAM emissions. Their analysis,

which assumed R-X mode emission with sources located just above the R-X cutoff frequency (f_{RX}), indicated that the wave normal angle at the source point decreased with increasing ratio of f/f_{RX} at the source point. Hashimoto and Goldstein match the occurrence probability of DAM emission in the Io-CML phase plane with three-dimensional ray tracing results for three different initial wave normal angles. Their results indicate that wave normal angle, $\Psi \approx 85°$ at the source point produced the best agreement with ground-based observations. Menietti et al., 1984 have performed three-dimensional ray tracing of DAM emissions and directly compared their results to Voyager observations. They point out that for a source region located just above the R-X cutoff frequency and for an initial wave normal angle close to 90°, there is good qualitative agreement with Voyager data. It appears (e.g. Goldstein and Thieman (1981) and Menietti et al., 1984) that high-curvature arcs such as those shown in Figure 1 cannot be reproduced with the initial wave normal angle equal to the same constant value at all frequencies, even when the refractive effects of the Jovian ionosphere are included. The ionospheric model introduced by Hashimoto and Goldstein (1983) together with the Acuna and Ness O-4 magnetic field model will affect northern hemisphere sources at mid to high latitudes only for $f > 20$ MHz. Ionospheric refraction cannot explain the low frequency refraction necessary to produce the observed signature of the high-curvature arcs.

In this paper, three-dimensional ray tracing is used to examine variable wave normal angle effects on the resulting DAM arc structure at frequencies just above the R-X cutoff and with several assumed ratios of f/f_g at the source point. We use whatever wave normal angle is necessary to match Voyager observations of two intense, vertex-late, high-curvature DAM arcs. The results indicate that one possible explanation of the double-valued frequency nature of the high-curvature arcs is Doppler-shifted gyroemission from a beam of electrons with $E \approx 10$ keV.

An independent investigation of Doppler-shifted gyroemission utilizing the results of Staelin (1981) has allowed us to set an approximate upper limit on the Doppler shift of the stimulating electrons. Wave normal angles which fall in the range of the ray tracing results, i.e. $\Psi_{MAX} > 70°$ are possible for Doppler-shifted gyroemission for $f/f_g > 1.1$ only if $V_\parallel/V > .7$ and $V_\parallel/c > .32$. This work represents the first comprehensive three-dimensional ray tracing investigation of varying the wave normal angle and Doppler shift utilizing realistic Jovian plasma and magnetic field models with direct comparison of the results to Voyager observations of DAM arcs. It thus complements and extends the results of Goldstein and Thieman (1981) and the work of Hashimoto and Goldstein (1983).

The ray tracing code used in this study has been described by Menietti et. al., (1984) so only a brief description will be given here. The code is three-dimensional and based on the cold plasma formulation of Stix (1962) and integrates the Haselgrove (1955) equations. The magnetic field model is the O-4 model (Acuna and Ness, 1976) and the plasma model is that introduced by Sentman and Goertz (1977). The three-dimensional results reduce to the two-dimensional results of Green et. al. (1977), Green and Gurnett (1980), and Lecacheux (1981).

The assumed emission mechanism requires that: (1) the radiation is R-X mode; (2) the source region is at the foot of the instantaneous Io flux tube and the frequency of the emission in the source region is greater than the RX cutoff frequency, and (3) the emission cone is hollow.

High-Curvature Arcs

Often seen in the Voyager PRA data are high-curvature arcs extending over time intervals of thirty minutes or more with frequency ranges of less than 1 MHz to over 30 MHz, (Figure 1 for example). These arcs occur isolated and

nested in groups. Two examples of isolated high-curvature arcs are shown plotted in Figure 2. These were observed by Voyager 1 on day 72 of 1979 and by Voyager 2 on day 188 of 1979. In order to model this class of arc the wave normal angle, Ψ, (the angle between $\overline{K}$ and the magnetic field, $\overline{B}$) was varied at the source point for each chosen frequency. Source points were chosen at a set of frequencies: 2, 5, 10, 15, 20, 25, and 30 MHz from the condition $f/f_g = 1.02$ and $f/f_g = 1.2$. These ratios were chosen to be consistent with Doppler-shifted emission at large wave normal angles. Gyroemission is not assumed for the ray tracing. The condition $f > f_{RX}$ was satisfied at each source point. For a specific frequency, ratio f/f_g, and sub-Io longitude (Io flux tube) an initial angle, Ψ, was chosen to begin ray tracing and the proximity of the resulting ray path to the spacecraft position (already known from observation of a particular high-curvature arc) was noted. If the resulting ray path did not intersect the spacecraft position, a new initial wave normal angle, Ψ, was chosen and the process repeated. A new Io flux tube was chosen for each frequency in agreement with observations because Io revolves slightly relative to Jupiter during the time of observation of an arc. The longitude of the currently stimulated Io flux tube was chosen according to observations. Since the observed arcs were treated as input constraints to the ray tracing process, this procedure generated model arcs which exactly matched the observed arcs when Ψ varied with frequency according to the curves shown in Figures 3 and 4.

Results

The results for the two high-curvature arcs observed by Voyager 1 on day 72 of 1979 and on day 188 of 1979 are shown in Figures 3 and 4 respectively. As can be seen, the $\Psi(f)$ curves for each modelled arc are qualitatively similar (peaking at $f \approx 10$ MHz and falling off at lower and higher frequencies). The curves of Figure 3 were evaluated for $f/f_g = 1.02$ and 1.2 at the source

points. An increase in the Doppler shift from $f/f_g = 1.02$ to $f/f_g = 1.2$ shifts the curve downward approximately 3° while the characteristic shape is maintained. The data for day 188 in Figure 4 for $f/f_g = 1.2$ and $f/f_g = 1.02$ show the same general functional relationship between Ψ and f as shown in Figure 3. In Figure 4 the shift in the curves is approximately 8° at the highest frequency. The arc vertex frequency (~ 10 MHz) requires the largest wave normal angle (~ 79°) at $f/f_g = 1.02$ as determined for both day 72 and day 188.

For both high-curvature arcs plotted in Figure 2 the Io flux tube intersects Jupiter at a longitude where the azimuthal variation in the B-field (O-4 model) is slight. The results may be explained by noting that since the source positions for the highest frequencies along the Io flux tube are closer to the planet by about 1 R_J, increased refraction of the higher frequencies refracts the emission cones so that the spacecraft observes the higher frequencies "inside" the emission cones of the lower frequencies (cf. Goldstein and Thieman, 1981).

Doppler-Shift Gyroemission Discussion

Let us consider the case of Doppler-shifted gyroemission from high energy, field-aligned electrons. The ray tracing analysis is not dependent on an emission mechanism and so this section is distinct from the ray tracing results. Staelin (1981) has used the results of Goldreich and Lynden-Bell (1969) to obtain an expression for the maximum wave normal angle expected for Doppler-shifted R-X emission (assuming the emission phase velocity is approximately equal to c) as

$$\Psi_{MAX} \approx \cos^{-1} \left\{ \frac{\left| \gamma \{f_p / f_g\}^2 + \gamma - 1 \right|}{K\{\gamma^2 - 1\}^{1/2}} \right\} \qquad (1)$$

where $K = V_{\parallel}/V$ and γ is the relativistic term. The Doppler-shifted frequency is given by

$$\frac{f}{f_g} = 1 + \frac{V_{\parallel}}{C} \cos\left(\frac{\pi}{2} - \frac{V_{\parallel}}{C}\right) \qquad (2)$$

For a given ratio, $V_{\parallel}/c$, the above equation 2 yields the Doppler shift ratio, f/f_g. Then, for a given value of K, γ is determined and Ψ_{MAX} can be found. The precise values of K and $V_{\parallel}$ appropriate for Jupiter are unknown. Using $V_{\parallel} \approx .1c$ (as Staelin suggests is consistent with observed decametric S burst frequency drifts) and choosing an intermediate value of $K \approx .5$ gives $\gamma = 1.02$ and $\Psi_{MAX} \approx 78°$ (if we assume $f_p/f_g << 1$ which is the case near most of the source points considered). This value of Ψ_{MAX} is close to the value of the peak wave normal angle shown in Figures 3 and 4 for $f/f_g = 1.02$. Figure 5 contains a family of Ψ_{MAX} versus K curves for values of $V_{\parallel}/c$ which vary from 0.1 to 0.45. This figure differs from Figure 2 of Staelin (1981) in that we have labelled curves as a function of the assumed Doppler shift ratio as shown in Table I. The value of γ varies slightly for each curve as shown. These curves demonstrate that the larger Doppler shifts (as shown in curves 4 and 5 for $f/f_g = 1.1$ and $f/f_g = 1.2$ respectively) produce values of $\Psi_{MAX} > 70°$ consistent with the ray tracing results shown in the curves of Figures 3 and 4 only if $K > .7$ and $V_{\parallel} > .32c$. Accepting $V_{\parallel} \approx .1c$ as a reasonable value, our results indicate that $f/f_g \approx 1.1$ is an upper limit to the Doppler shift at the source point for the arcs considered in this study.

TABLE 1

PARAMETERS USED IN FIGURE 5

Curve	f/f_g	$V_\parallel/c$	γ_{min}	γ_{MAX}
1	1.01	0.10	1.01	1.03
2	1.02	0.14	1.01	1.04
3	1.04	0.20	1.02	1.09
4	1.10	0.32	1.05	1.12
5	1.20	0.45	1.10	1.20

Conclusions

In the Voyager PRA data set one frequently observes either isolated or nested groups of arcs that have a larger curvature and are difficult to explain if one assumes Ψ = constant ≈ 90°. Two examples of isolated, vertex-late, high-curvature arcs have been matched through ray tracing by allowing the wave normal angle to vary with frequency. The $\Psi(f)$ relationship that produced these spectral features was peaked around 10 MHz and fell off on either side in qualitative agreement with the earlier two-dimensional ray tracing results of Goldstein and Thieman (1981).

If a gyroemission mechanism is assumed that produces Doppler-shifted emission, the results of Staelin (1981) predict a frequency dependence of the wave normal angle. An energetic, field-aligned electron beam ($v_\parallel$ = 0.1c) could produce maximum wave normal angles in agreement with those found in the present models if $f/f_g \approx 1.02$ and $K \approx 0.5$. Such energies (10 keV) are comparable to suggested energies of several keV for accelerated electrons near the surface of Io which may be the source of DAM emission (cf. Shawhan, 1976; Goldstein and Goertz, 1983). We emphasize, however, that our ray tracing results are not

dependent on a gyroemission mechanism. Each of the $\Psi(f)$ curves were obtained from ray tracing by requiring that the model DAM high-curvature arcs matched those observed by Voyager 1 on day 72 (Figure 3) and day 188 (Figure 4) of 1979. The characteristic shape of the curves (with a peak at the vertex frequency) does not significantly change as the Doppler shift increases. The wave normal angle, Ψ, varies between 70° and 80° for all Doppler shifts considered with smaller values of Ψ resulting from larger assumed Doppler shifts. Independent of the ray tracing results, the condition that gyroemission occur for $f > f_{RX}$ (equation 1 [cf. Staelin, 1981]) suggests that an electron beam with $K \approx .5$ and $V_{\|} \approx .1c$ will result in Ψ_{MAX} which agrees favorably with the results shown in Figures 3 and 4. Figure 5 and the values listed in Table 1 indicate that larger Doppler shifts ($f/f_g \approx 1.1$ and $f/f_g \approx 1.2$) will produce $\Psi_{MAX} > 70°$ in agreement with the ray tracing results only for $K > .7$ and $V_{\|}/c \geq .35$. The value of $K = V_{\|}/V$ appropriate for Jupiter is not known. But observations of frequency drifts of Jovian S bursts imply that $V_{\|} \approx .1c$. As seen from Table 1 this implies that for the two high-curvature arcs presently modelled, curves 1 and 2 for $V_{\|}/c \leq .14$ and $f/f_g \approx 1.02$ best match the ray tracing results. The two arcs presently modelled were chosen because of the large frequency dispersion and intense emission. We believe these arcs represent emission at close to the smallest wave normal angles and the largest Doppler shifts for observed DAM arcs (Figures 3 and 4 indicate that a larger assumed Doppler shift at the source point yields a smaller value of Ψ_{MAX}). Our results thus indicate that $f/f_g \approx 1.1$ is the largest to be expected for Jovian DAM arcs, with typical values being $f/f_g \leq 1.02$. While we have chosen only vertex-late arcs for this investigation (due to the intensity of the emission and large frequency dispersion) we expect no differences in our conclusions for the vertex-early arcs. We have excluded radiation from Alfven wave reflections located away from the Io flux tube. If

simultaneous emission from multiple flux tubes was responsible for the production of the two isolated arcs modelled, our conclusions would have to be modified.

ACKNOWLEDGEMENTS

The authors are indebted to Dr. James Warwick and the Planetary Radio Astronomy team (in particular M. Kaiser) for the use of the Voyager 1 and 2 time averaged PRA calibrated data. This research was supported by the National Aeronautics and Space Administration under the Jupiter Data Analysis Program, (NASA contract NAS7-100) through Cal Tech/JPL contract 956026. The authors would also like to express their gratitude to the Data System Technology Program for allowing access to the central computer facilities through the Space Plasma Computer Analysis Network (SCAN).

REFERENCES

Acuna, M. H., and Ness, N. F., "Results from the GSFC Fluxgate Magnetometer on Pioneer 11", Jupiter, ed. T. Gehrels, 1976, pp. 830-847.

Boischot, A., A. Lecacheux, M. L. Kaiser, M. D. Desch, J. K. Alexander, and J. W. Warwick, "Radio Jupiter after Voyager: An Overview of the Planetary of the Planetary Radio Astronomy Observations", J. Geophys. Res., 86, 8213, 1981.

Green, J. L., D. A. Gurnett, and S. D. Shawhan, "The Angular Distribution of Auroral Kilometric Radiation", J. Geophys. Res., 82, 1825, 1977.

Green, J. L. and D. A. Gurnett, "Ray Tracing of Jovian Kilometric Radiation", Geophysical Research Letters, 7, 65, 1980.

Green, J. L., "The Io Decametric Emission Cone", Radio Scienc, 19, 556-570, 1984.

Goldreich, P. and D. Lynden-Bell, "Io, A Jovian Unipolar Inductor", Astrophys. J., 1956, 59, 1969.

Goldstein, Melvyn L. and J. R. Thieman, "The Formation of Arcs in the Dynamic Spectra of Jovian Decametric Bursts", 86, 8569, 1981.

Goldstein, Melvyn L. and C. K. Goertz, "Theories of Radio Emissions and Plasma Waves", in Physics of the Jovian Magnetosphere, ed. A. J. Dessler, 1983.

Haselgrove, J., "Ray Theory and a New Method of Ray Tracking", London Physical Society, Report on Conference on the Physics of the Ionosphere, 1955, pp. 355-364.

Hashimoto, J. and M. L. Goldstein, "A Theory of the Io Phase Assymmetry of the Jovian Decametric Radiation", J. Geophys. Res., 88, 2010, 1983.

Lecacheux, Alain, "Ray Tracing in the Io Plasma Torus: Application to the PRA Observastions During Voyager 1's Closest Approach", J. Geophys. Res., 86, 8523, 1981.

Menietti, J. D., J. L. Green, S. Gulkis, and N. F. Six, "Three Dimensional Ray Tracing of Jovian Decametric Arcs, J. Geophys. Res., 89, 1489-1495, 1984.

Sentman, D. C. and C. K. Goertz, "Whistler Mode Noise in Jupiter's Inner Magnetosphere", J. Geophys. Res., 83, 322, 1977.

Shawhan, S. D., "Io Sheath-Accelerated Electrons and Ions", J. Geophys. Res., 81, 3373, 1976.

Staelin, David H., "Character of the Jovian Decametric Arcs", J. Geophys. Res., 86, 8581, 1981.

Stix, T. H., The Theory of Plasma Waves, McGraw-Hill Book Co. Inc., 5-34, 1962.

Figure Captions

Fig. 1. Frequency-time spectrograms of Voyager low-frequency radio emissions. The emission intensity is gray-shade coded acording to the bar graph at the left. In the top panel low-curvature DAM arcs observed by Voyager 1 on day 197 of 1979 are seen from about 0510 UT to about 0550 UT. In the bottom panel is seen a typical example of a high-curvature DAM arc obsrerved by Voyager 1 on day 72 of 1979 and extending from about 1150 UT to arc vertex at about 1235 UT.

Fig. 2. A frequency versus system-III longitude plot of Voyager data for two observed isolated DAM high-curvature arcs: Voyager 1 for day 72 of 1979 (shown in spectrogram in Figure 1); and Voyager 2 for day 188 of 1979.

Fig. 3. Initial wave normal angle, Ψ, versus frequency obtained from ray tracing which resulted in a DAM arc identical in curvature to that observed by Voyager 1 on day 72 of 1979. The upper curve is for an initial Doppler-shift of $f/f_g = 1.02$, while the lower curve is for $f/f_g = 1.2$.

Fig. 4. Same format as Figure 3 except for comparison to the arc observed by Voyager 2 on day 188 of 1979.

Fig. 5. Maximum wave normal angle, Ψ_{MAX}, versus K $(V_\parallel/V)$ for a family of curves with parameters varying as shown in Table 1. The ratio, f/f_g, increases from 1.01 (curve 1) to 1.2 (curve 5). Gamma is approximately a constant for each curve.

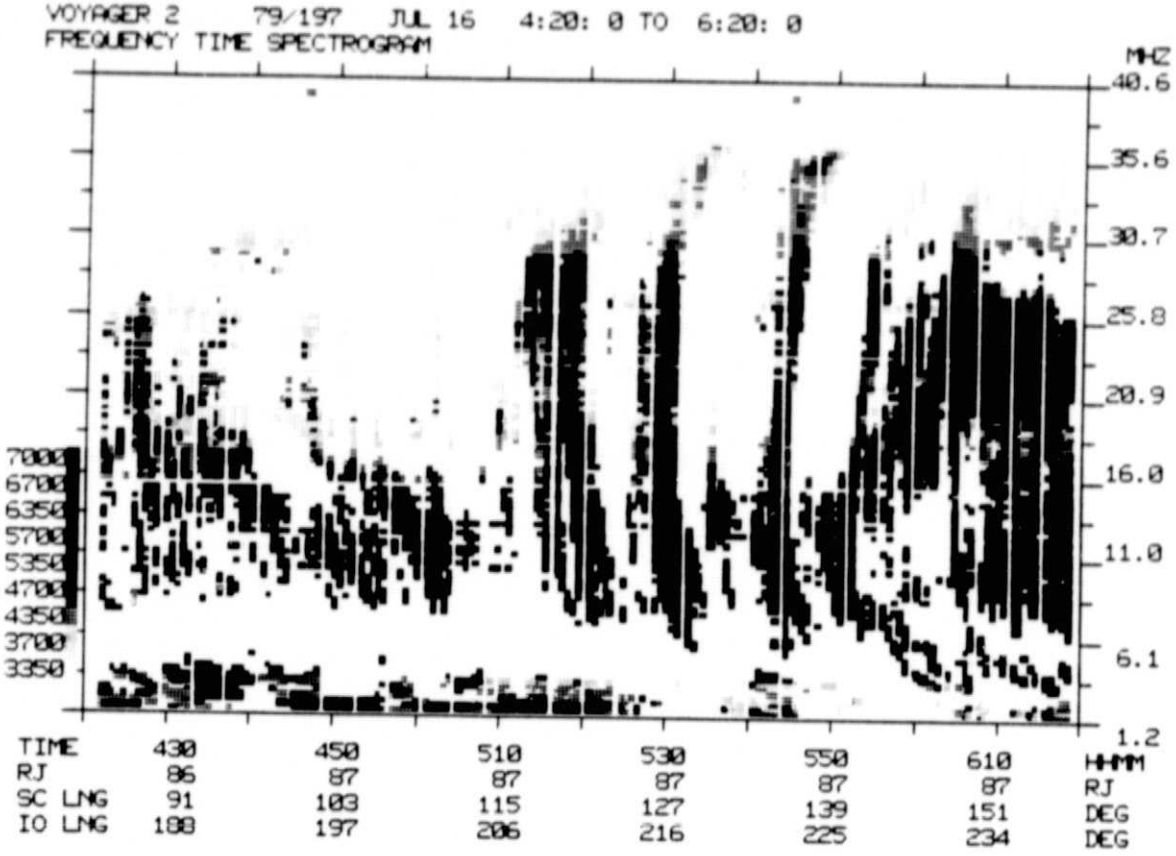
VOYAGER 2 79/197 JUL 16 4:20: 0 TO 6:20: 0
FREQUENCY TIME SPECTROGRAM
MHZ
40.6
35.6
30.7
25.8
20.9
16.0
11.0
6.1
1.2
7000
6700
6350
5700
5350
4700
4350
3700
3350
TIME 430 450 510 530 550 610 HHMM
RJ 86 87 87 87 87 87 RJ
SC LNG 91 103 115 127 139 151 DEG
IO LNG 188 197 206 216 225 234 DEG

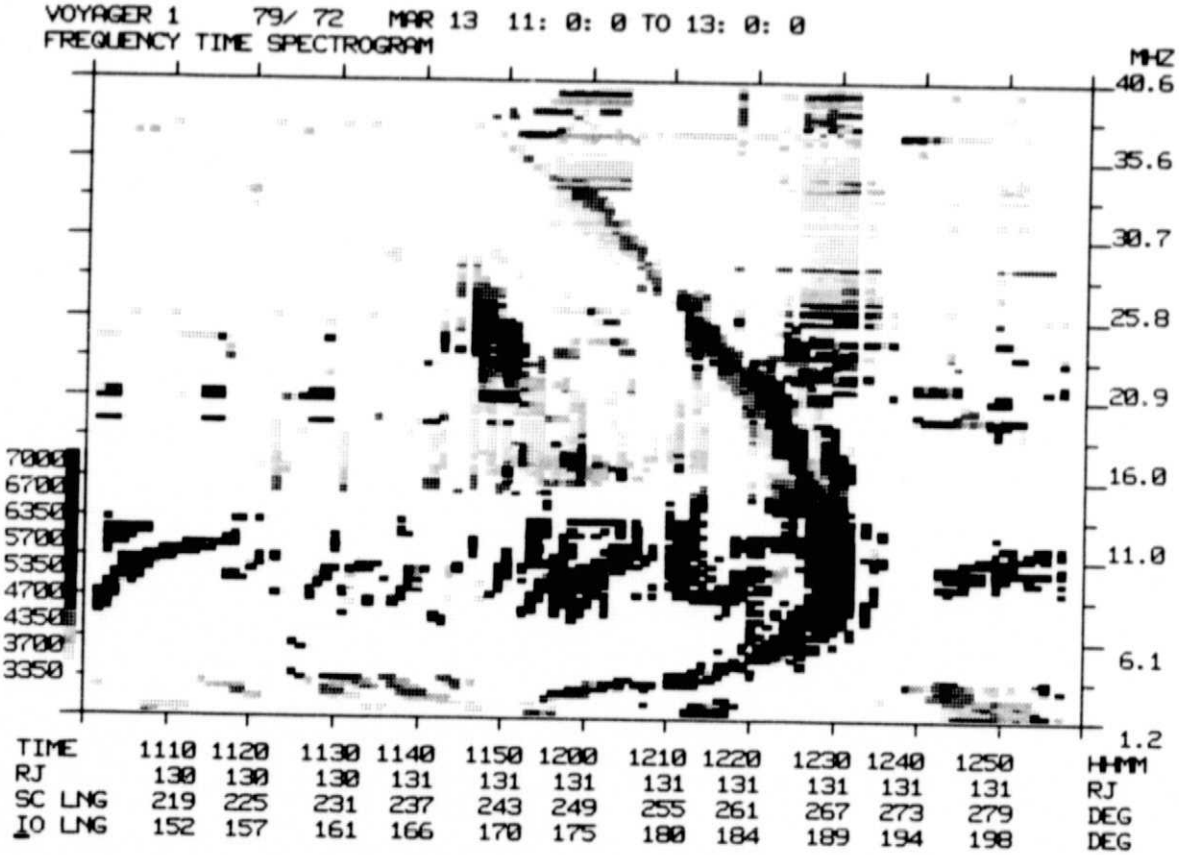
VOYAGER 1 79/ 72 MAR 13 11: 0: 0 TO 13: 0: 0
FREQUENCY TIME SPECTROGRAM
MHZ
40.6
35.6
30.7
25.8
20.9
16.0
11.0
6.1
1.2
7000
6700
6350
5700
5350
4700
4350
3700
3350
TIME 1110 1120 1130 1140 1150 1200 1210 1220 1230 1240 1250 HHMM
RJ 130 130 130 131 131 131 131 131 131 131 131 RJ
SC LNG 219 225 231 237 243 249 255 261 267 273 279 DEG
IO LNG 152 157 161 166 170 175 180 184 189 194 198 DEG

FIGURE 1

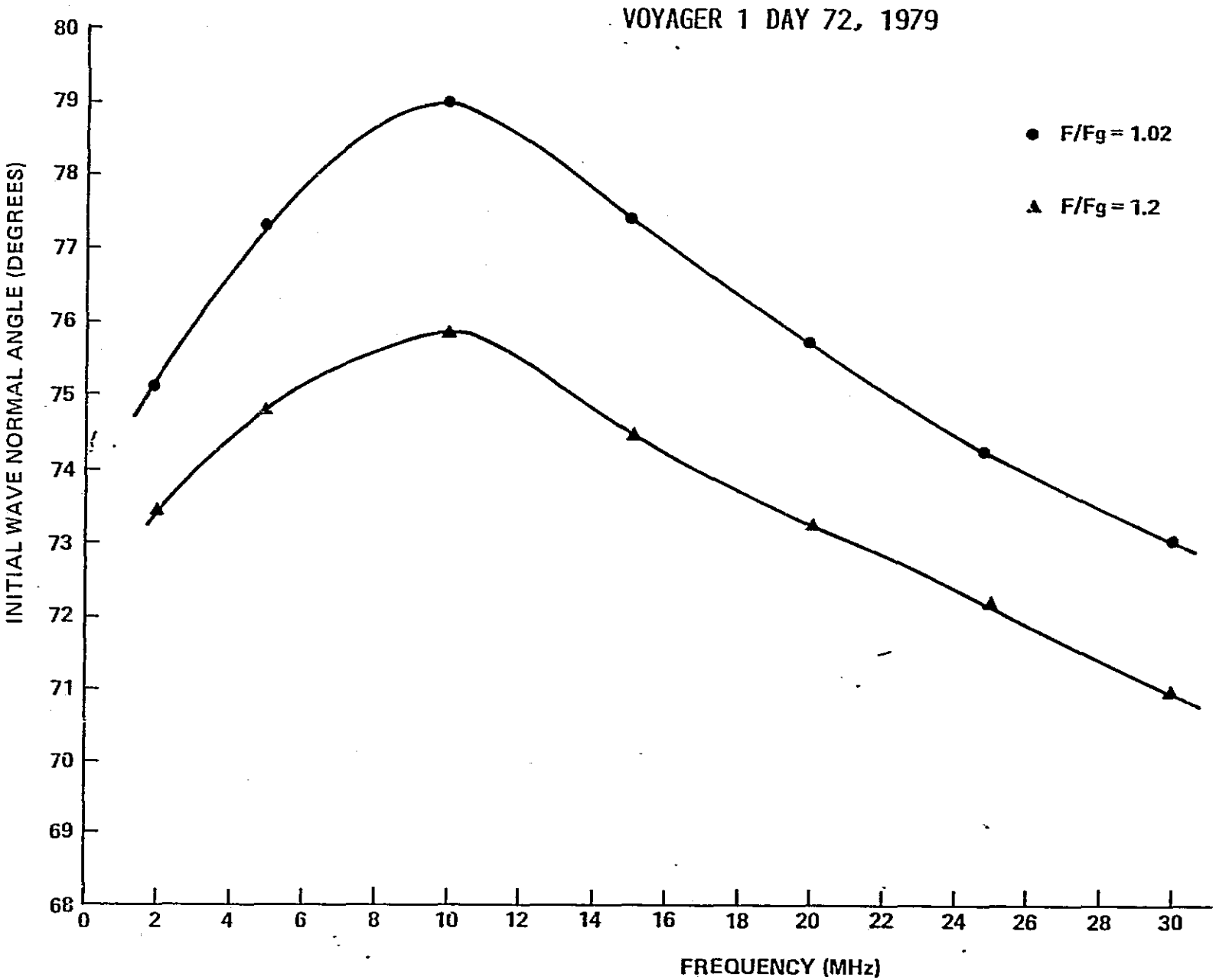
VOYAGER 1 DAY 72, 1979
INITIAL WAVE NORMAL ANGLE (DEGREES)
80
79
78
77
76
75
74
73
72
71
70
69
68
F/Fg = 1.02
F/Fg = 1.2
0
2
4
6
8
10
12
14
16
18
20
22
24
26
28
30
FREQUENCY (MHz)

FIGURE 3

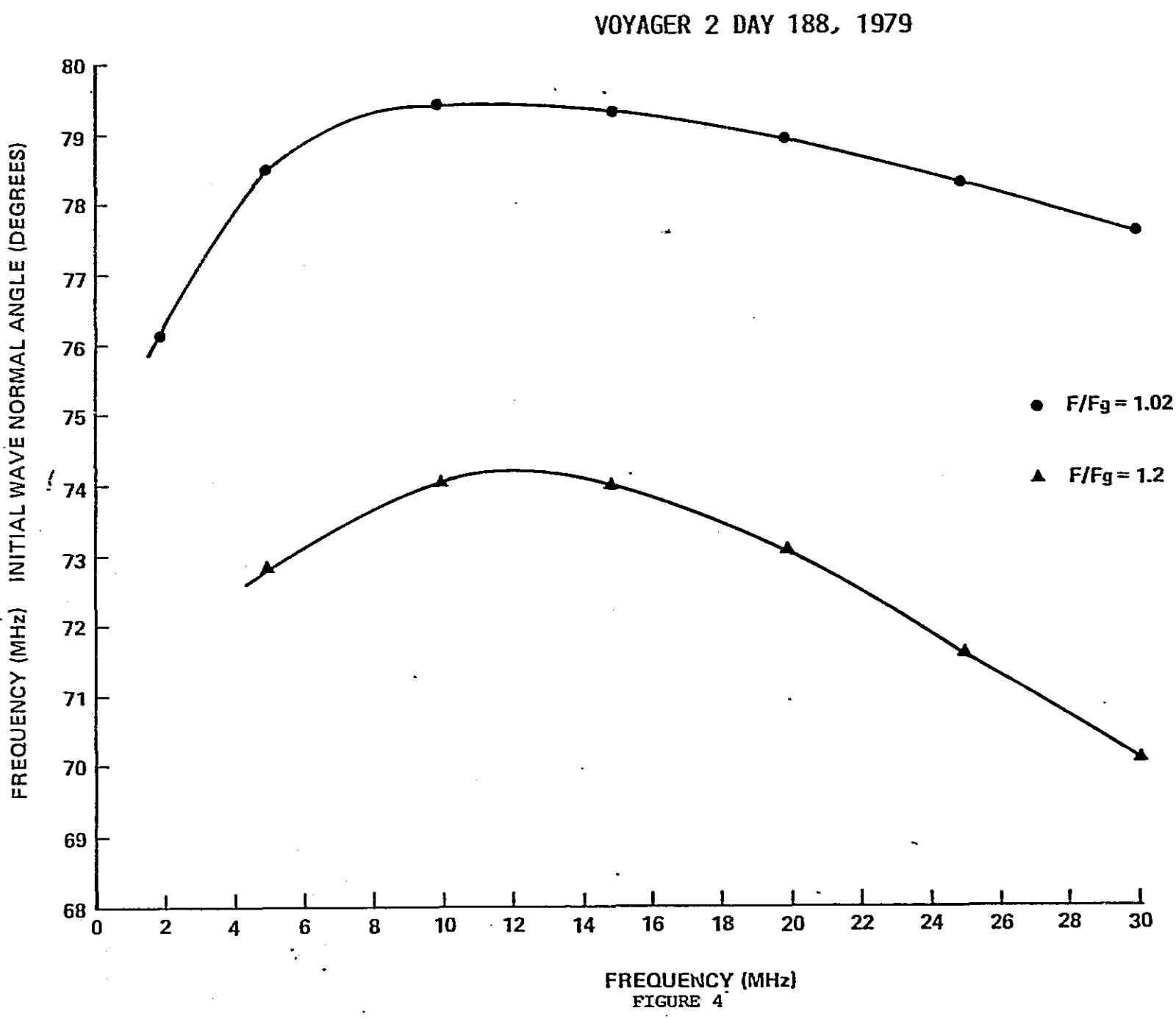
VOYAGER 2 DAY 188, 1979
FREQUENCY (MHz) INITIAL WAVE NORMAL ANGLE (DEGREES)
80
79
78
77
76
75
74
73
72
71
70
69
68
0
2
4
6
8
10
12
14
16
18
20
22
24
26
28
30
F/Fg = 1.02
F/Fg = 1.2
FREQUENCY (MHz)

FIGURE 4

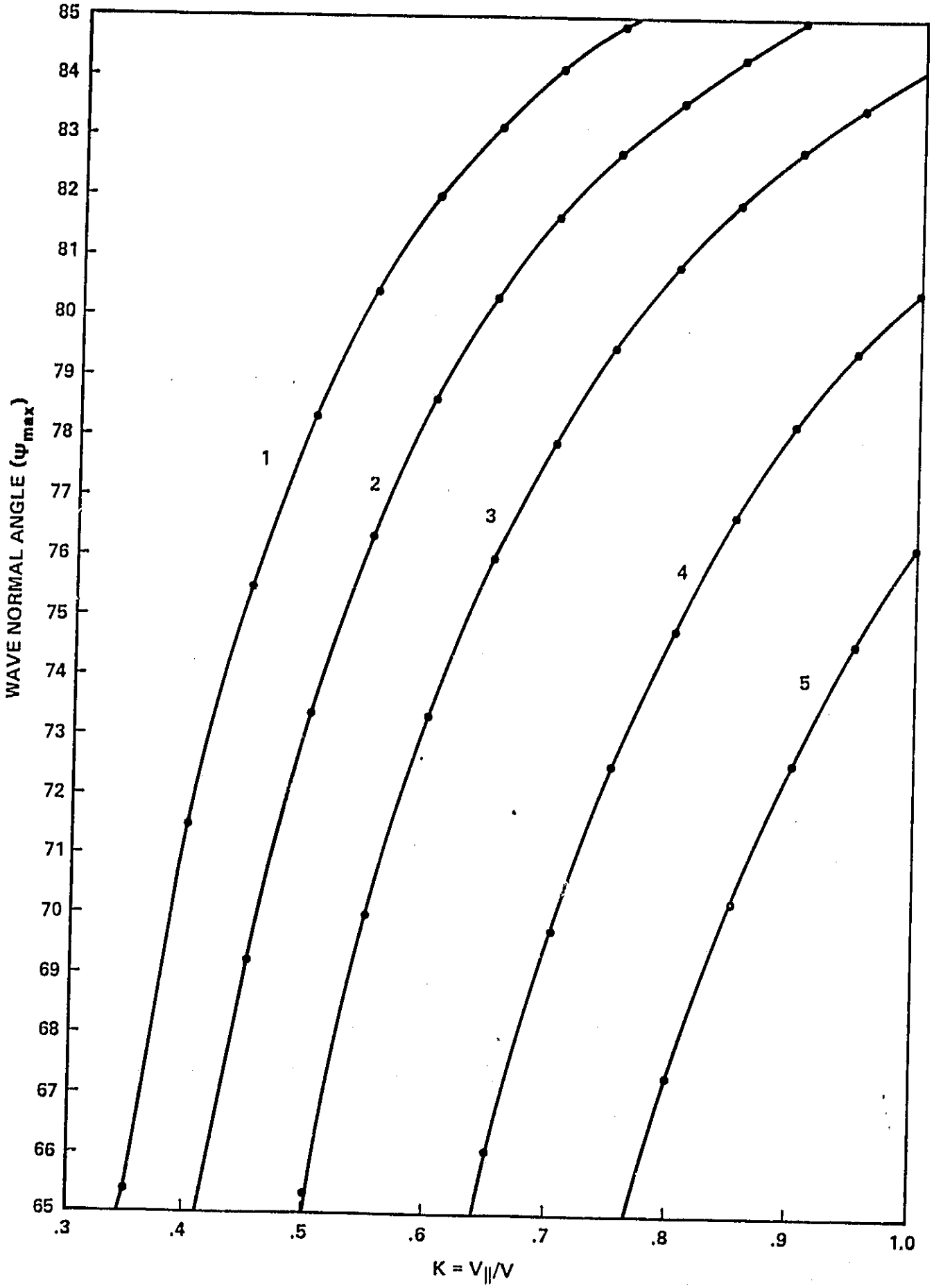
WAVE NORMAL ANGLE (ψ_{max})
85
84
83
82
81
80
79
78
77
76
75
74
73
72
71
70
69
68
67
66
65
1
2
3
4
5
.3
.4
.5
.6
.7
.8
.9
1.0
K = $V_{||}/V$

FIGURE 5

D. Appendix 4: "Identification of a Night-Side Component of DAM as a Jovian Counterpart to AKR"

IDENTIFICATION OF A NIGHT-SIDE COMPONENT OF DAM AS A JOVIAN COUNTERPART TO AKR

BY

James Lauer Green
Magnetospheric Physics Branch
Space Science Laboratory
NASA/Marshall Space Flight Center, AL 35812

N. Frank Six *
Western Kentucky University
Bowling Green, Kentucky

Sam Gulkis
Jet Propulsion Laboratory
Pasadenia, California

J. D. Menietti
Southwest Research Institute
San Antonio, Texas

December 1983

Submitted to the Journal of Geophysical Research

* Now at Arecibo Observatory
Arecibo, Puerto Rico

ABSTRACT

The post-encounter Voyager detection of a night-side decametric emission which differs from pre-encounter and earth-based observations is examined in this study. This intense radiation is observed in the frequency range from about 12 to 25 MHz, is detected in bursts lasting a couple of hours, is localized in Jovian longitude, and is clearly an Io phase independent emission. A spatial survey of this emission reveals that it is observed when the Voyager spacecraft are in the System III (1965) longitude range from 150 to nearly 190 degrees, at positive magnetic latitudes, and with a local time from 0 to 3.9 hours on the night-side of the planet. The night-side nature of this emission prevented its detection by Earth-based radio observations which are made in the local time range from about 11.3 to 12.7 hours.

This night-side component of decametric radiation may be coming from the low-altitude night-side auroral zone which is linked to the Jovian plasmasheet by magnetic field lines that are at higer latitudes than Io's field lines. From all indications, it appears that this emission is the Jovian counterpart to the Earth's auroral kilometric radiation or AKR, hence it is referred to here are Jovian Auroral Decametric Radiation or JADR. Since JADR is seen nearly every time the Voyager spacecraft are in the emission pattern of the radiation, the night-side Jovian tail field auroral zone may be continuously active.

INTRODUCTION

It is clear from satellite and Earth-based observations that the Jovian magnetosphere provides a rich environment for the generation of many types of free escaping radio emissions. Earth-based radio measurements as early as 1955 discovered emission from Jupiter at decametric or DAM wavelengths.

Brigg discovered in 1964 that the phase of Io has a strong influence on whether or not decametric radio emissions from Jupiter are detected at earth. This Io effect has led to the classification of the decametric emissions as Io dependent and Io independent. The Io independent emissions are less intense and show Jovian longitude control.

This paper will discuss observations from the PRA experiment onboard the Voyager 1 and 2 spacecraft of a new type of Io independent emission at decametric wavelengths which shows a strong dependence on the observing longitude and magnetic latitude and are seen only on the night-side of Jupiter.

OBSERVATIONS

In order to concentrate on the Io independent emissions close examination of the data must be made to clearly identify the Io dependent emissions. Decametric measurements have been routinely put into a coordinate system of central meridian longitude (CML) versus Io phase (see for example Alexander et al., 1981). In this coordinate system Io dependent emissions have been classified as "sources" or regions of CML and Io phase where the probability of measuring decametric radiation is high. It has been known for sometime that the most intense decametric emissions are from sources A, B, and C. Green, 1984 using Voyager 1 and 2 observations over several months organized the Voyager data into spacecraft-Io longitude difference versus frequency for fixed positions of Io in System III ('65) longitute. As discussed in detail in Green, 1984 the purpose of plotting the Voyager data in this new coordinate system is to eliminate the relative motion of Jupiter and Io. The result of the coordinate transformation of the Voyager data (see Figures 3, 4, 5, and 6 of Green, 1984) is the same as would be observed by a spacecraft that moved completely around Jupiter at a constant radial distance keeping Io and Jupiter fixed. It is important to note that out of several months of observations only a relatively small amount of data is used which satisfied the conditions of having Io at a specified system III longitude.

The analysis presented here carries the work of Green, 1984 a step further by selecting a band of frequencies for each fixed Io sorted data plot of spacecraft-Io longitude difference (or phase) (in this case from 15 to 21 MHz). Figure 1 presents the occurrence of decametric emission in the frequency range 15 to 21 MHz over the period June 26 to July 23, 1979 versus Io longitude. The top panel is determined from all PRA observations on the inbound and outbound leg of the Voyager 2 flyby. A $1/R^2$ factor was used to take into account the radial dependence of the emission. An occurrence block is shown when the average decametric intensity (normalized to 10 R_j) over the 15 to 21 MHz frequency range was greater than 1.1×10^{-17} Watts/ m^2/Hz. Observations closer than 30 R_j to the center of Jupiter were not used to avoid any possible propagation effects in the inner Jovian magnetosphere. All spacecraft observations are organized in longitude bins 3 degrees wide and plotted such that Io's position is along a vertical line at the center of the plot, with the difference between spacecraft longitude and Io longitude increasing to the right of center and decreasing to the left of center. Along the ordinate the data is organized into 6 degree wide Io longitude increments spaced every 10 degrees apart. Labeled in all three panels of Figure 1 are the expected locations of the Io dependent sources A, B, and C. Vertical features on these plots would maintain constant Io-observer phase and hence, be labeled "Io phase dependent". Note that periodic observations of decametric radiation are seen extending

from the upper left corner of Figure 1 (top panel) to the lower right. Although these observations cross into the B source it is certain that they are not Io phase dependent.

The middle and bottom panels of Figure 1 are plotted in the same format as the top panel, but contain only inbound data (middle panel) and outbound data (bottom panel) data. When the Voyager 2 data are separated in this manner, incomplete sampling occurs at many of the longitudes. The regions of no observations in this coordinate system are shown shaded. The separation of the Voyager 2 data into inbound and outbound passes is performed in order to examine the local time effects in the observation of the periodic decametric radiation pointed out in the top panel. The PRA measurements on the inbound portion of the Voyager flybys restrict the majority of the observations to the day-side Jovian magnetosphere from 9.5 to 11.0 hours local time (LT) and the outbound from 0 to 2.8 hours LT. A comparison between the middle and bottom panels indicates that the periodic emission seen in the top panel extending from upper left to lower right is observed only on the outbound leg of the Voyager 2 flyby. This analysis confirms the detection of a night-side component of decametric emission from Jupiter, which is clearly Io phase independent.

The spectrogram of Figure 2 shows the frequency-time characteristics of a typical night-side decametric burst lasting a couple of hours. The enhancement in decametric emission at the low frequencies, from about 8 to 16 MHz, may be attributed to an increase in sensitivity of the PRA instrument in this frequenc

range recently determined by Schauble and Carr, 1983. The enhanced sensitivity in this frequency range sometimes gives the appearance that a broad Jovian emission band exits. In order to avoid the sensitivity effect and to provide a concise picture, the entire frequency range of the night-side decametric emission was not used (only frequencies from 15 to 21 MHz were used) in the determination of DAM occurrence of Figure 1. Usually in the 8 to 16 MHz frequency range, "arc" structures (see Warwick et al., 1979a and Leblanc, 1981) are found that are typical of non-Io emissions, however, in Figure 2, at higher frequencies (>12 MHz) this emission is not made up of a series of arcs and is much broader (as observed in time) than a single arc. The frequency-time structure of this emission is seen periodically in the Voyager 2 observations from about 25 R_j until the emission is just barely measured above the receiver's noise level at distances greater than 120 R_j.

The spectral characteristics of the night-side decametric emission of Figure 2 is shown in Figure 3 where the power flux emission (expressed in Watts/m^2/Hz) has been normalized to 10 R_j. In addition, Figure 3 shows only the maximum power flux observed at each frequency over the spacecraft longitude range from 150 to 160 degrees (about 17 minutes of data). Note that this emission reaches peak intensity from 14 to 25 MHz and decreases rapidly at higher and lower frequencies. This spectral shape is not characteristic of the Io dependent decametric

emission (Carr et al., 1983) but it does more closely resemble the spectral shape of the Earth's auroral kilometric radiation (see for example Gurnett, 1974).

The repetition of the night-side decametric bursts may be understood by examining if there is any dependence on the spacecraft position in magnetic latitude and longitude for observing the emission. On a "wiggle" plot (position in magnetic latitude and radial distance with time), of the Voyager 2 outbound trajectory in Figure 3, are dark strips where complete night-side decametric bursts are observed. These bursts are observed exclusively at high positive magnetic latitudes with the high frequencies seen at magnetic latitudes greater than about 9 degrees. It is important to note that the highest frequencies of the night-side decametric emission (20 to 22 MHz) are not measured when the spacecraft is at the highest magnetic dipole latitude (corresponding to approximately 200 degrees longitude) but at the latitude which corresponds to the longitude (about 150 degrees) of the believed maximum surface magnetic field strength (see for example, Connerney, et al., 1981). This relationship is very suggestive of low altitude source regions which have a strong dependence on Jupiter's magnetic field. In addition, since the maximum frequency is observed at or very near the longitude of the maximum field strength the beaming of this emission appears to nearly parallel to the magnetic field in the source region. This situation is very different from the broad emission cones (large initial wave normal angles) that are believed to be so characteristic of the Io A and B sources (s

Green, 1984). Better understanding of the emission and propagation characteristics of this radiation is currently under study using ray tracing techniques.

The spatial distribution of the night-side DAM as suggested by Figure 1 can be further investigated by using Voyager 1 PRA data as well as the Voyager 2. The Voyager outbound trajectories, looking down from the north onto an equatorial plane, are plotted in Figure 5. The shaded regions are at the position of the spacecraft where the night-side DAM was measured. The cross hatched block at the expected location of the emission along the Voyager 2 trajectory is due to the inability to clearly separate the night-side DAM emission from intense Io dependent source B radiation measured at the same time. It is important to note however, that the Voyager 1 measurements of the night-side DAM abruptly stopped after a radial distance of about 58 R_j and local time of 3.9 hours. The Voyager 2 observations of this emission, shown in Figure 5, continue until the intensity of the emission is near the PRA experiment noise level at radial distances greater than 120 R_j. The overall repetition of the Voyager 2 observations (and to some extent the Voyager 1) strongly indicates that the absence of Voyager 1 night-side DAM observations past 58 Rj on the outbound trajectory is due to a spatial and not temporal effect and that the this emission has a distinct outer boundary that Voyager 1 passed through. Combined with the results of Figure 4, the "inner boundary" labeled in Figure 5 is probably due to the low magnetic latitude measurements near the encounter.

DISCUSSION

The night-side DAM emission reported here has been commented on in the paper by Alexander et al., 1981. This emission, as described here, can be easily seen in the synoptic analysis of Plate 1 in the Alexander et al., 1981 paper for only the Voyager 2 after encounter plot with traces of the emission seen in the Voyager 1 after encounter data. The low occurrence probably of the night-side DAM from the Voyager 1 observations in the Alexander et al., 1981 paper is undoubtably due to the fact that Voyager 1 was in the emission region for only a short time (see Figure 4 of this paper). Alexander et al., 1981 did point out that the "Io-independent emission at frequencies above 20 MHz exhibit marked local time effects". Their interpretation of this emission as a feature which "probably corresponds to the weak Io-independent B source recorded in earth-based surveys" is not the interpretation presented here. It is without question that the night-side DAM can only be measured at high magnetic latitudes (greater than 9 degrees) and on the night-side of Jupiter, both of which, the Earth-based measurements are unable to achieve. The situation with the lower frequency extension of this emission (less than 12 MHz) however is not at all clear and may very well be related to the Io-independent B source as discussed by Alexander et al., 1981. Additional work needs to be done to clarify this point.

From the above observations it is important to compare the night-side DAM to other well known magnetospheric emissions in order to gain insight on its possible origin and generation. It is generally believed that the earth's auroral kilometric radiation (AKR) is the terrestrial counterpart to the decametric radiation from Jupiter. These emissions have many physical similarities such as the same polarization, the same frequency range when normalized with respect to the planets magnetic field, high latitude low altitude source regions, and the most intense free escaping radio frequency radiation generated in their respective magnetospheres. Many generation mechanisms have been proposed for both AKR and DAM which are the same (see for example Melrose, 1976). However, when considering the Io control of the intense DAM radiation there is no obvious terrestrial counterpart. A more analagous comparison would be between AKR and the Io independent emissions. The night-side DAM emissions, discussed here, are the only Io independent emission which have spatial and spectral characteristics similar to AKR. The angular distribution of AKR has been extensively studied (see Green et al., 1977, for example) and it is clear that AKR emission exhibits latitudinal propagation effects and is seen primarily on the night-side of the earth. If the night-side DAM is the Jovian counterpart to AKR, then it may be coming from Jupiter's tail field auroral zone (with low altitude sources) which is at higher latitudes than the field lines that Io intersects (Connerney, et al., 1981). Because of these similarities, the night-side decametric emissions will be referred to here as

Jovian Auroral Decametric Radiation or JADR. The persistence of JADR in the Voyager 2 data may therefore indicate that Jupiter has an extremely active and continuous night-side particle precipitation in the Jovian tail-field auroral zone. It is important to note that recent work by Maeda and Carr, 1984 suggests that the Io-independent A source, seen on the day-side of the Earth, may have an Jovian auroral zone origin. How this emission relates to the JADR discussed here is not known and it is hoped that future ray tracing studies may be successful in determining the relationship between the Io-independent A source and JADR.

CONCLUSIONS

We have presented an identification of one of the decametric components generated in the Jovian magnetosphere. This emission, referred to here as JADR, has been measured by the Voyager 1 and 2 PRA experiments and has the following major characteristics:

1. JADR is an Io-phase independent emission in the frequency range from 12 to 25MHz.

2. JADR (from 16 to 25MHz) cannot be categorized as having an "arc" like structure characteristic of much of the Io-dependent and -independent emissions.

3. The JADR power spectrum is not typical of the Io-dependent or Io-independent DAM emissions.

4. There is a strong latitudinal and longitudinal beaming of JADR since it is observed at positive magnetic latitudes with the highest frequencies measured when the largest surface magnetic field strength (near 150 degrees) is near the longitude meridian of the spacecraft.

5. It is observed only on the outbound portions of the Voyager flyby trajectories.

6. A strong night-side beaming effect is implied when an abrupt halt to intense JADR observations from Voyager 1 occurs at local times greater than 3.9 hours, while Voyager 2, at local times less than 2.8 hours observes the emission to radial distances greater than 120 R_j.

A number of conclusions can be made from the observed characteristics of the JADR emissions and their similarity to other magnetospheric emissions. These include:

1. A possible propagation effect may be responsible for the magnetic latitude asymmetry seen.

2. Any southern hemisphere JADR emissions would only be observed at the lowest frequency (12 MHz) since neither Voyager 1 or Voyager 2 were at southern magnetic latitudes greater than about 7 degrees.

3. JADR emission may be the Jovian counterpart to the earth's auroral kilometric radiation and emanate from a continuously active Jovian tail field auroral zone.

ACKNOWLEDGMENTS

The authors are indebted to Dr. James Warwick and the Planetary Radio Astronomy team (in particular M. Kaiser) for the use of the Voyager 1 and 2 time averaged PRA calibrated data. This research was supported by the National Aeronautics and Space Administration under the Jupiter Data Analysis Program. The authors would also like to express their gratitude to the Data System Technology Program for allowing access to the central computer facilities through the Space-plasma Computer Analysis Network (SCAN).

REFERENCES

1. Alexander, J.K., T.D. Carr, J.R. Thieman, J.J. Schauble, and A.C. Riddle, Synoptic observations of Jupiter's Radio Emissions: Average statistical properties observed by Voyager, J. Geophys. Res., 86, 8529, 1981.

2. Bigg, E.K., Influence of the satellite Io on Jupiter's decametric emission, Nature, 203, 1008, 1964.

3. Connerney, J.E.P., M.H. Acuna, and N.F. Ness, Modeling the Jovian Current Sheet and Inner Magnetosphere, J. Geophys. Res., 86, 8370, 1981.

4. Carr, T.D., M.D. Desch, and J.K. Alexander, Phenomenology of magnetospheric radio emission, in Physics of the Jovian Magnetosphere, Edited by A. J. Dessler, pp. 226-284, Cambridge University Press, New York, 1983.

5. Green, J.L., D.A. Gurnett, and S.D. Shawhan, The Angular Distribution of Auroral Kilometric Radiation, J. Geophys. Res., 82, 1825, 1977.

6. Green, J.L., The Io Decametric Emission Cone, to be published in Radio Science, April 1984.

7. Gurnett, D. A., The Earth as a Radio Source: Terrestrial Kilometric Radiation, J. Geophys. Res., 79, 4227, 1974.

8. Leblanc, Y., On the arc structure of the DAM Jupiter emission., J. Geophys. Res., 86, 8564, 1981.

9. Maeda, K. and T. D. Carr, Beam Structure of Jupiter's Decametric Radiation, to be published in Nature, 1984.

10. Melrose, D. B., An interpretation of Jupiter's decametric radiation and the terrestrial kilometric radiation as direct amplified gyroemission, Astrophys. J., 207, 651, 1976.

11. Schauble, John J. and Thomas D. Carr, Calibration of the Voyager Planetary Radio Astronomy Radiometers above 4 MHz, Paper presented at the National Radio Science Meeting, Boulder, Colorado, January 6, 1983.

12. Warwick, J.W., J.B. Pearce, A.C. Riddle, J.K. Alexander, M.D. Desch, et al., Voyager 1 Planetary Radio Astronomy Observations Near Jupiter, Science, 204, 995, 1979a.

Figure 1

Occurrence of DAM emission from Voyager 2 spacecraft is shown by the blacken squares when the average intensity is greater than 1.1×10^{-17} Watts/m^2/Hz. (normalized to 10 R_j) over the frequency range from 15 to 21 MHz. This three panel figure is derived from observations taken along the outbound (bottom), inbound (middle), and both inbound and outbound (top) Voyager 2 trajectory. The DAM occurrences are plotted in degree difference between the spacecraft and Io versus Io System III ('65) longitude. In the top and bottom panels only, a systematic DAM non-Io emission is observed from the upper left to the lower right corner of the plot.

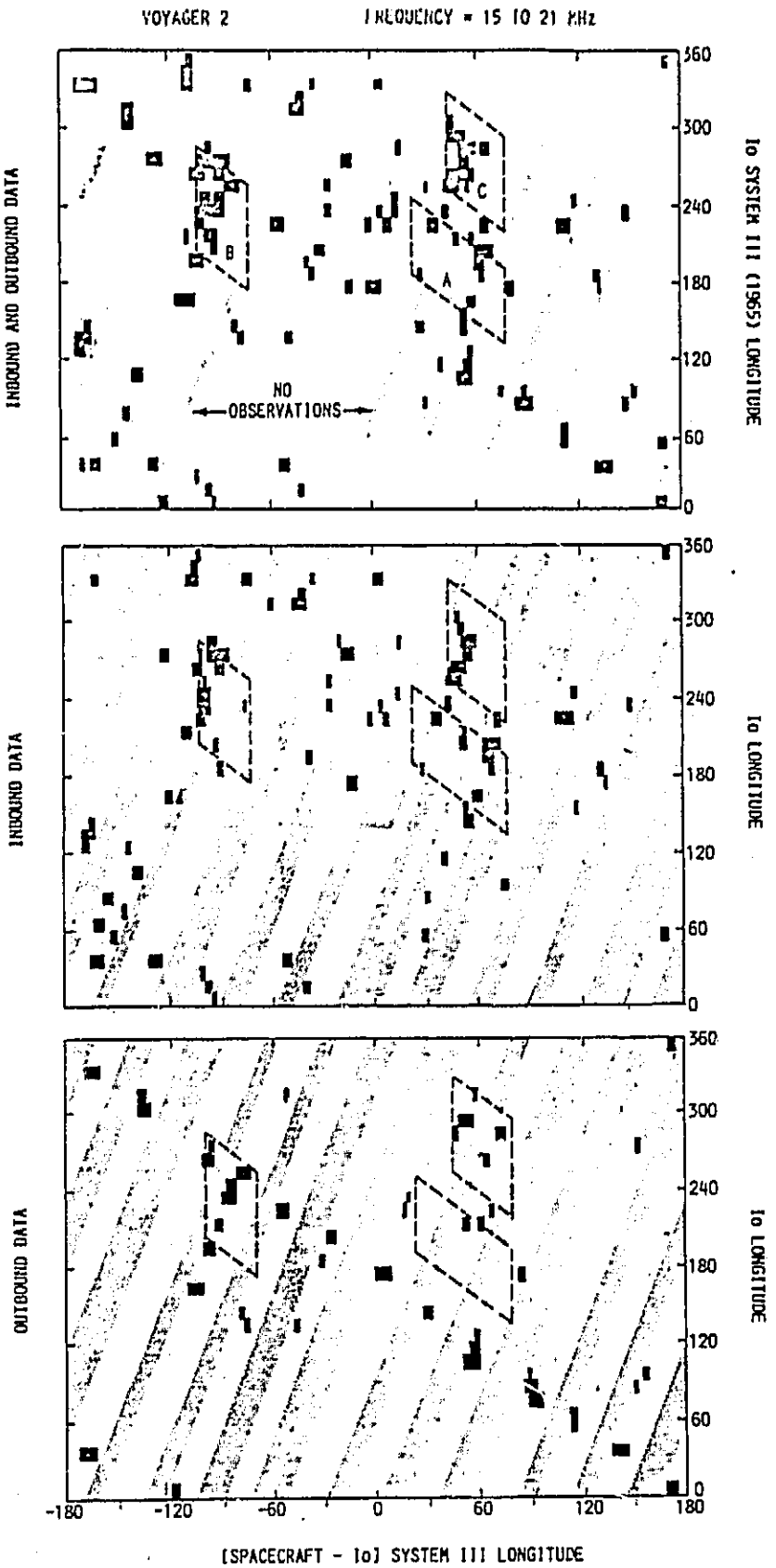
VOYAGER 2
FREQUENCY = 15 TO 21 MHz
INBOUND AND OUTBOUND DATA
INBOUND DATA
OUTBOUND DATA
NO OBSERVATIONS
A
B
C
Io SYSTEM III (1965) LONGITUDE
Io LONGITUDE
0
60
120
180
240
300
360
-180
-120
-60
0
60
120
180
[SPACECRAFT - Io] SYSTEM III LONGITUDE

Figure 1

Figure 2

This Voyager 2 frequency-time spectrogram shows the basic characteristics of the JADR emissions. A night-side decametric burst usually lasts about an hour and is first seen in Voyager 1 and 2 data at high frequencies (typically 21 to 22 MHz) and as a function of time to lower and lower frequencies until a broad emission band appears from 8 to 12 MHz.

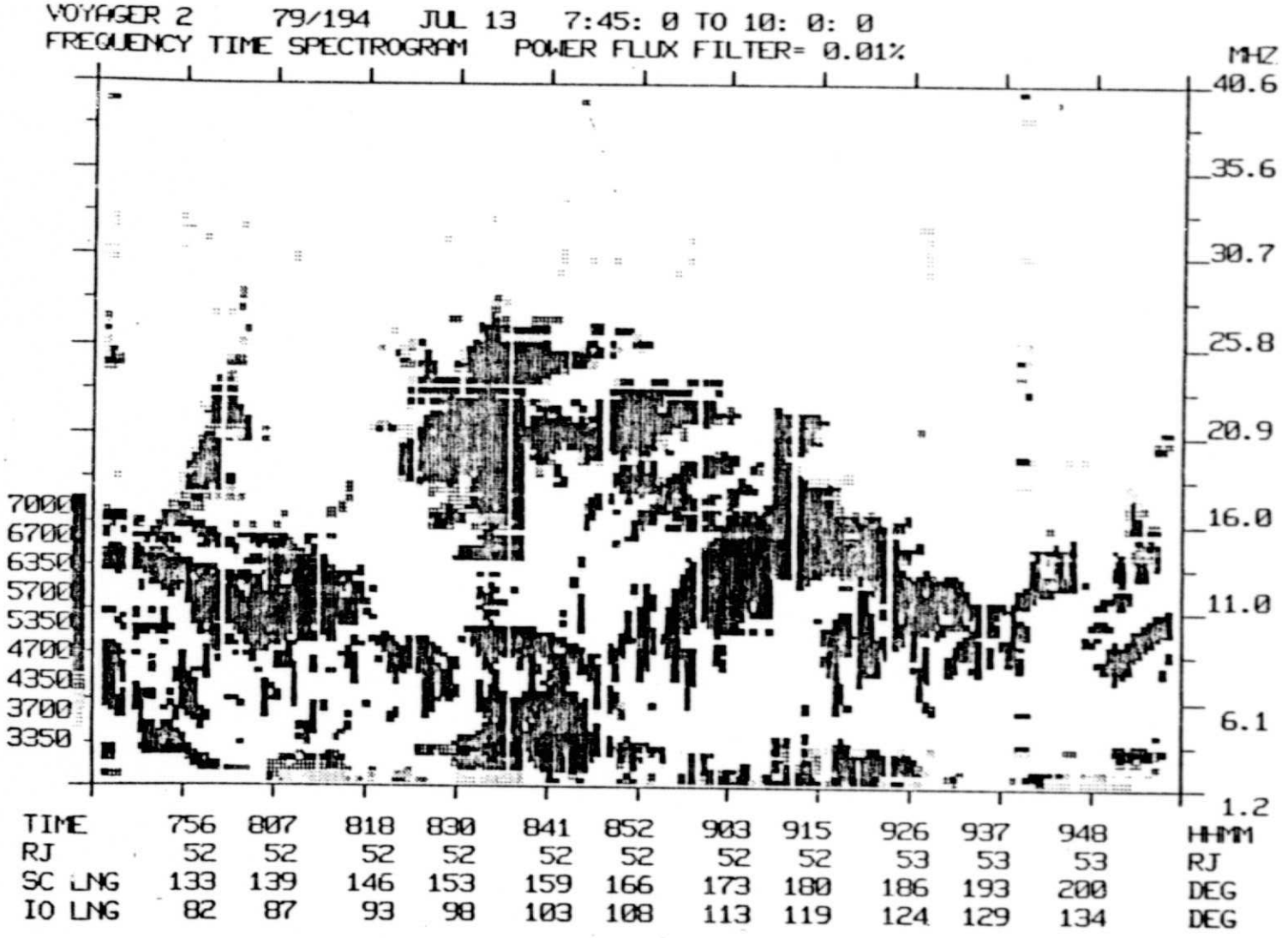
VOYAGER 2 79/194 JUL 13 7:45: 0 TO 10: 0: 0
FREQUENCY TIME SPECTROGRAM POWER FLUX FILTER= 0.01%
MHZ
40.6
35.6
30.7
25.8
20.9
16.0
11.0
6.1
1.2
7000
6700
6350
5700
5350
4700
4350
3700
3350
TIME 756 807 818 830 841 852 903 915 926 937 948 HHMM
RJ 52 52 52 52 52 52 52 52 53 53 53 RJ
SC LNG 133 139 146 153 159 166 173 180 186 193 200 DEG
IO LNG 82 87 93 98 103 108 113 119 124 129 134 DEG

Figure 2

Figure 3

The maximum power flux spectrum of the night-side decametric emission is shown in this figure. Note that the spectral peak occurs from 14 to 22 MhZ and rapidly decreases at higher and lower frequencies.

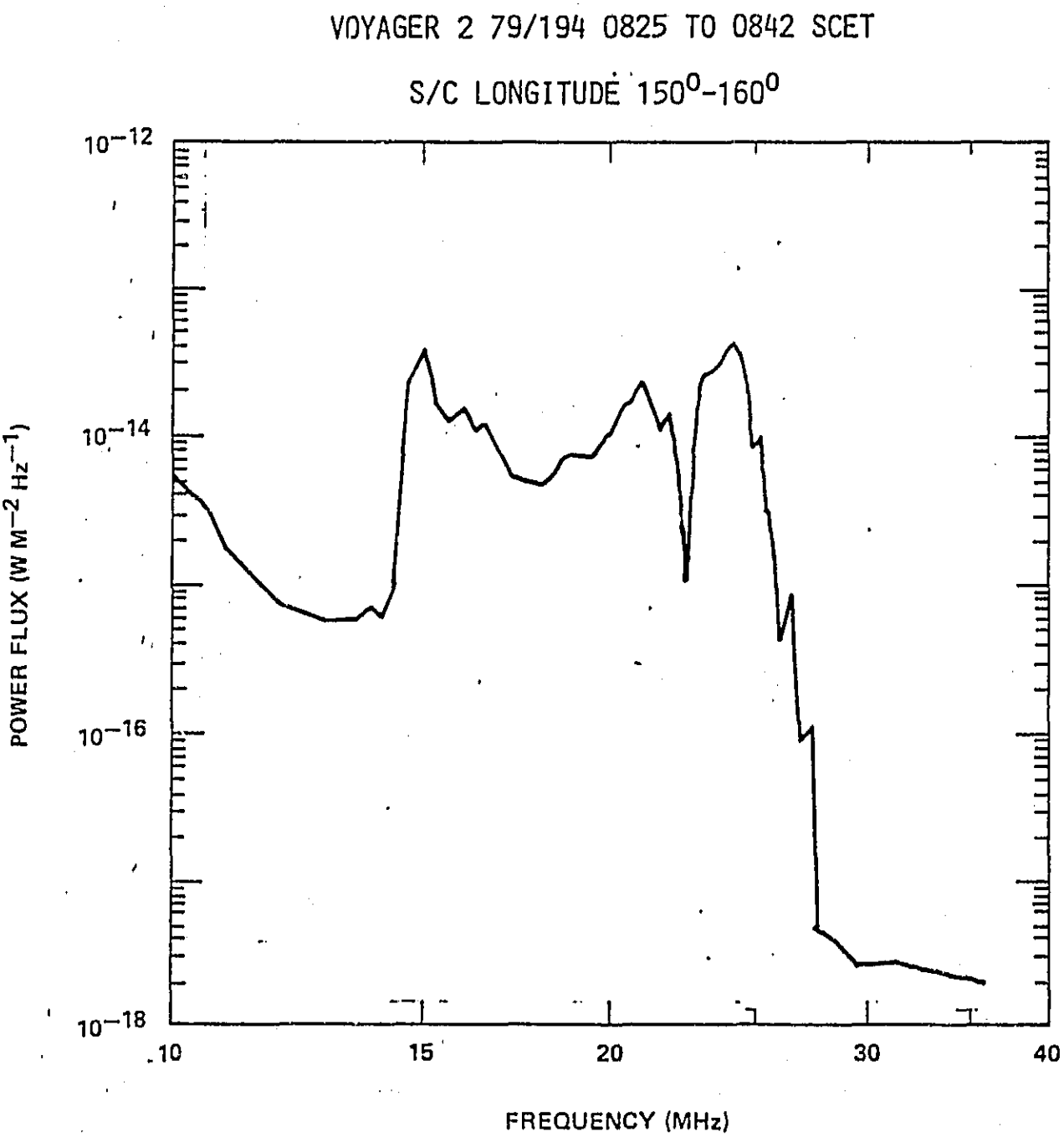
VOYAGER 2 79/194 0825 TO 0842 SCET
S/C LONGITUDE 150°-160°
POWER FLUX (W M⁻² Hz⁻¹)
10⁻¹²
10⁻¹⁴
10⁻¹⁶
10⁻¹⁸
10
15
20
30
40
FREQUENCY (MHz)

Figure 3

Figure 4

The position of the Voyager 2 spacecraft when the night-side DAM emissions are observed in magnetic latitude and radial distance coordinates are shown here as darkened strips during the outbound portion of its trajectory. The characteristic shape of these emissions as pointed out in Figure 2 were used in determining the spacecraft positions of the shaded strips. Note that the night-side DAM emissions are all seen at positive magnetic latitudes with the highest frequencies observed near the beginning of each strip.

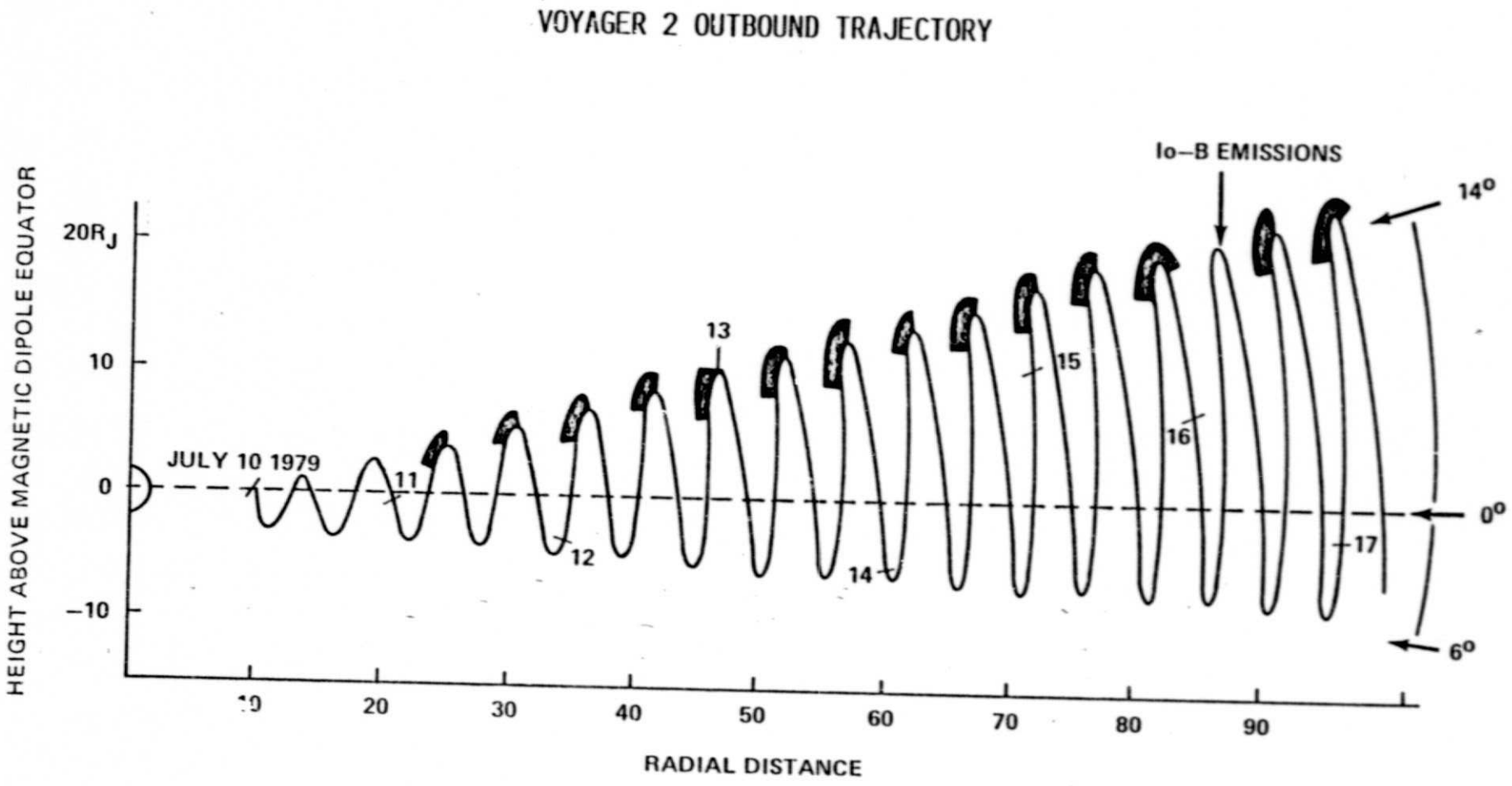
VOYAGER 2 OUTBOUND TRAJECTORY
Io–B EMISSIONS
14°
0°
6°
HEIGHT ABOVE MAGNETIC DIPOLE EQUATOR
20R_J
10
0
−10
JULY 10 1979
11
12
13
14
15
16
17
20
30
40
50
60
70
80
90
RADIAL DISTANCE

Figure 4

Figure 5

The dark block regions along the outbound Voyager 1 and 2 near equatorial trajectories show the position of the spacecraft when the night-side DAM was observed. Note that there are only a few examples of this emission observed from Voyager 1. The crossed hatched area is near the expected location for the night-side DAM but its characteristic frequency-time structure cannot be clearly distinguished from other decametric emissions which are measured at that time. The Voyager 2 spacecraft observed the night-side DAM to radial distances greater than 100 R_j (not shown in this figure) just above the receiver noise level. The wavy lines represent qualitative boundaries of the emission based on these observations.

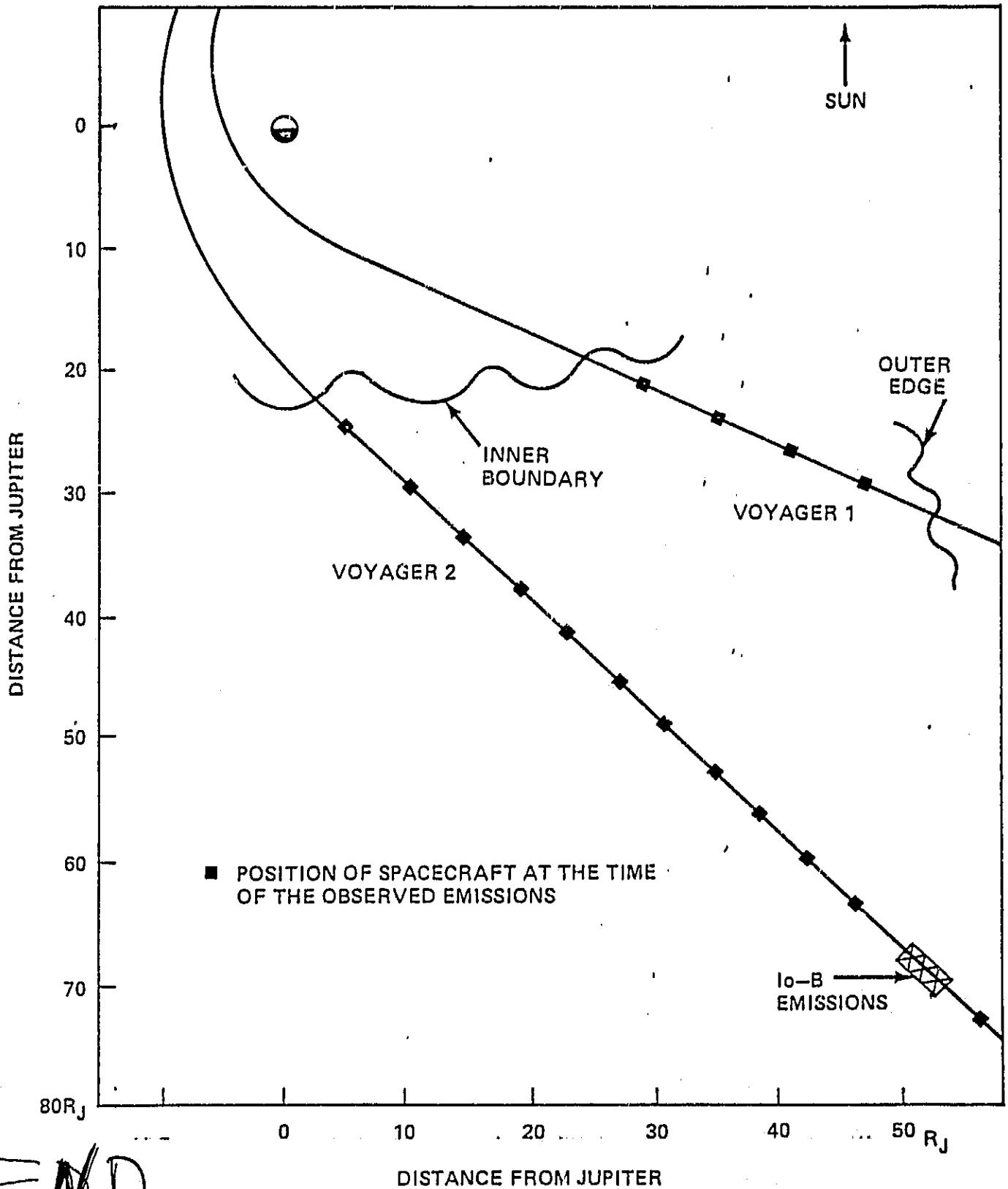

END DATE APR. 26, 1985

Figure 5